

**Analytical results for $e^+e^- \rightarrow t\bar{t}$ and $\gamma\gamma \rightarrow t\bar{t}$ observables
near the threshold up to the next-to-next-to-leading
order of NRQCD.**

A.A.Penin*

*Institut für Theoretische Teilchenphysik Universität Karlsruhe
D-76128 Karlsruhe, Germany*

A.A.Pivovarov*

*Institut für Physik, Johannes-Gutenberg-Universität
D-55099 Mainz, Germany*

Abstract

We present the analytical description of top-antitop pair production near the threshold in e^+e^- annihilation and $\gamma\gamma$ collisions. A set of basic observables considered includes the total cross sections, forward-backward asymmetry and top quark polarization. The threshold effects relevant for the basic observables are described by three universal functions related to S wave production, P wave production and $S - P$ interference. These functions are computed analytically up to the next-to-next-to-leading order of NRQCD. The total $e^+e^- \rightarrow t\bar{t}$ cross section near the threshold is obtained in the next-to-next-to-leading order in the closed form including the contribution due to the axial coupling of top quark and mediated by the Z -boson. The effects of the running of the strong coupling constant and of the finite top quark width are taken into account analytically for the P wave production and $S - P$ wave interference.

PACS numbers: 14.65.Ha, 13.85.Lg, 12.38.Bx, 12.38.Cy

*On leave from Institute for Nuclear Research, Moscow, Russia

1 Introduction.

Being heavy the top quark undergoes fast weak decays. The relatively large width Γ_t of the top quark is mainly saturated by the decay channel $t \rightarrow Wb$ and keeps the effective energy of top-antitop system in the complex plane far enough from the cut along the positive semiaxis. Thus it serves as a sufficient infrared cutoff for long distance effects avoiding the problem of strong coupling. This allows one to bypass possible nonperturbative regions and is the key observation for the theoretical study of the top-antitop pair production near the two-particle threshold [1]. Because the relevant scale $\sqrt{\Gamma_t m_t}$, with m_t being the top quark mass, is much larger than Λ_{QCD} , the QCD perturbation theory expansion is applicable for the theoretical description of physical phenomena near the top quark threshold if singular Coulomb effects are properly taken into account [1, 2, 3]. This feature turns the processes involving the top quarks into a unique laboratory for perturbative investigation of threshold effects. Experimental study of the top-antitop pair threshold production is planned to be performed at the Next Linear Collider both in high energy e^+e^- annihilation and $\gamma\gamma$ collision [4]. High quality experimental data that can be obtained in such experiments along with a very accurate theoretical description of them make the processes of top-antitop pair threshold production a promising place for investigating quark-gluon interactions. This investigation concerns both general features of interaction and precise quantitative properties such as the determination of numerical values of the strong coupling constant α_s , the top quark mass, and the top quark width. Though the main features in both e^+e^- and $\gamma\gamma$ processes of top quark pair threshold production are rather similar the strong interaction corrections and relativistic corrections are different for them. Therefore a simultaneous analysis of these two processes extends possibilities of studying fine details of the top quark threshold dynamics. Besides the total cross sections which are mainly saturated by the S wave final state of the top quark-antiquark pair, there is a set of observables sensitive to the P wave component. For example, the S and P partial waves of the final state top quark-antiquark pair produced

in $\gamma\gamma$ collisions can be separated by choosing the same or opposite helicities of the colliding photons [2]. This gives an opportunity of direct measurement of the P wave amplitude which is strongly suppressed in the threshold region in comparison with the S wave one. On the other hand, the forward-backward asymmetry of the quark-antiquark pair production in e^+e^- annihilation [5, 6] and top quark polarization [6, 7] are determined by the $S - P$ wave interference in both processes. This provides us with two additional independent probes of the top quark interactions.

The finite order perturbation theory of QCD breaks down in the threshold region of particle production due to the presence of singular $(\alpha_s/\beta)^n$ Coulomb terms. Here β is a velocity of the heavy quark. However the resummation of these Coulomb contributions which are most important quantitatively in the threshold region is possible and can be systematically done in the framework of nonrelativistic QCD (NRQCD) [8] (for the recent development of the NRQCD effective theory approach see [9, 10, 11, 12, 13, 14, 15, 16]). Note that the characteristic scale of the Coulomb effects for the top quark production $\alpha_s m_t$ is comparable numerically with the cutoff scale for infrared effects $\sqrt{\Gamma_t m_t}$ so the Coulomb effects are not suppressed by the top quark width. The determination of higher order corrections in the QCD coupling constant and of relativistic corrections in the case when Coulomb effects have to be taken into account beyond the finite order perturbation theory requires the perturbative expansion for the complete correlator to be performed near the Coulomb approximation rather than near Green functions of the free theory which is the standard pattern of perturbation theory for the infrared safe high energy processes.

Recently has been made a rather essential progress in the theoretical description of heavy quark-antiquark threshold dynamics within NRQCD. The evaluation of next-to-leading order (NLO) and next-to-next-to-leading order (NNLO) corrections to the heavy quark threshold production in e^+e^- annihilation has been done both within the analytical approach [17, 18, 19, 20, 21, 22, 23, 24, 25] and numerically [26, 27, 28, 29, 30] while the NLO corrections

to the heavy quark threshold production in $\gamma\gamma$ collision where computed analytically [31]. The analysis of NNLO corrections in the last case is still absent. However, this analysis is necessary for the accurate quantitative study of the process since the NNLO contribution is found to be relatively large in the case of the top quark production in e^+e^- annihilation [26, 27] and one can expect that some large corrections emerge also in the case of the top quark threshold production in $\gamma\gamma$ collision. Moreover, a semianalytical analysis of the high order corrections to the top quark threshold production cross section in e^+e^- annihilation has been performed so far [26, 27, 29, 30] while the essential part of corrections has been accounted for numerically [3]. Therefore the complete analytical description of the process is also desirable¹. Furthermore, the forward-backward asymmetry and top quark polarization has been analyzed in NLO only numerically [6] as well as the axial contribution in the $e^+e^- \rightarrow t\bar{t}$ process [28]. In this case the numerical study is more involved because of necessity to construct the Green function for the P wave which leads to the more singular differential equations in comparison with the S wave. The case of P wave production in $\gamma\gamma$ collision [2, 31] clearly demonstrates that the numerical analysis [28] with an explicit cutoff of the hard momentum contribution is not sufficient for an accurate account for the finite top quark width for these quantities because the relativistic effects are not taken into account properly.

In the present paper we give a simultaneous analysis of several observables relevant to $e^+e^- \rightarrow t\bar{t}$ annihilation and $\gamma\gamma \rightarrow t\bar{t}$ collisions near the top quark production threshold in high orders of NRQCD. The total cross sections are computed in NNLO of NRQCD which includes α_s^2 , $\alpha_s\beta$ and β^2 corrections in the coupling constant α_s and the heavy quark velocity β to the nonrelativistic Coulomb approximation. Explicit analytical expressions for the soft part of corrections are obtained. The threshold cross section of the $t\bar{t}$ production in e^+e^- annihilation is obtained in the closed form including the contribution due to the top quark axial coupling. The hard part of the correction to the $\gamma\gamma \rightarrow t\bar{t}$ threshold cross section is

¹When this work was in its final stage a letter [22] appeared where the photon mediated top quark production in e^+e^- annihilation was analyzed analytically.

found with the logarithmic accuracy. The forward-backward asymmetry of the top quark-antiquark pair production in e^+e^- annihilation and top quark polarization in both processes of e^+e^- annihilation and $\gamma\gamma$ collisions are computed up to NLO.

The paper is organized as follows. In the next Section the nonrelativistic approximation for the basic observables of top quark-antiquark pair production near the threshold is formulated. In Section 3 the threshold effects are described by three universal functions related to the S , P wave production and $S - P$ wave interference which have been computed analytically within NRQCD. In Section 4 we present our numerical analysis and the discussion of the obtained results. The last Section is devoted to our conclusions. Some explicit analytical formulae are given in Appendix.

2 The nonrelativistic approximation near the production threshold.

In this section we describe the set of observable which will be analyzed: the total cross sections, the forward-backward asymmetry, the polarization of top quark. We formulate the nonrelativistic approximation for these observables setting the stage for the complete NRQCD analysis. In the last subsection we dwell upon the peculiarities of introducing the finite width of the top quark.

2.1 The effective theory description of the heavy quark threshold dynamics.

Near the threshold the heavy quarks are nonrelativistic so that one may consider both the strong coupling constant and heavy quark velocity as small parameters. The threshold expansion of the QCD loop integrals has been developed in [14]. However, to take into account the singular threshold effects properly one has to go beyond the finite order QCD

perturbation theory. For this purpose the expansion in β should be performed directly in the QCD Lagrangian within the effective field theory framework. The first step to construct the effective theory is to identify all the scales present in the problem. The threshold dynamics is characterized by four different scales [14]:

- (i) the hard scale (energy and momentum scale like m_q);
- (ii) the soft scale (energy and momentum scale like βm_q);
- (iii) the potential scale (the energy scales like $\beta^2 m_q$, while the momentum scales like βm_q);
- (iv) the ultrasoft scale (both energy and momentum scale like $\beta^2 m_q$). The ultrasoft scale is only relevant for gluons.

By integrating out the hard scale of QCD one arrives at the effective theory of NRQCD [8]. Because the NRQCD Lagrangian does not contain explicitly the heavy quark velocity the power counting rules are necessary to construct the regular expansion in this parameter. The list of the power counting rules for dimensionally regularized NRQCD and their relation to the threshold expansion [14] can be found in [16] Integrating out the soft modes and the potential gluons of NRQCD one obtains the effective theory of potential NRQCD [13] which contains potential quarks and ultrasoft gluons as active particles and is relevant for the analysis of the threshold effects. In potential NRQCD the dynamics of the quarks is governed by the effective nonrelativistic Schrödinger equation and by their interaction with the ultrasoft gluons. To obtain a regular perturbative expansion in β this interaction should be expanded in multipoles. Note that in the process of scale separation some spurious infrared and ultraviolet divergences may appear at intermediate steps of calculation which cancel each other in the final results for physical observables. The dimensional regularization has been recognized as a powerful tool to deal with these divergences [9, 12, 13, 14, 15, 16, 32, 33, 34, 35].

If the ultrasoft effects are neglected the propagation of a quark-antiquark pair in the color singlet state is described in the potential NRQCD by the Green function $G(\mathbf{x}, \mathbf{y}, E)$ of

the Schrödinger equation

$$(\mathcal{H} - E) G(\mathbf{x}, \mathbf{y}, E) = \delta(\mathbf{x} - \mathbf{y}) \quad (1)$$

where \mathcal{H} is the effective nonrelativistic Hamiltonian. Near the threshold the singular $(\alpha_s/\beta)^n$ Coulomb terms should be summed up in all orders in α_s . Thus, in threshold region one has to develop the expansion in β and α_s around some solution which incorporates properly the threshold effects, for example, around the nonrelativistic Coulomb solution. In this case the leading order approximation for the nonrelativistic Green function is obtained with the Coulomb Hamiltonian

$$\mathcal{H}_C = -\frac{\Delta_{\mathbf{x}}}{m_t} + V_C(x)$$

where $\Delta_{\mathbf{x}} = \partial_{\mathbf{x}}^2$ is the kinetic energy operator and $V_C(x) = -C_F\alpha_s/x$ is the Coulomb potential, $x = |\mathbf{x}|$. The harder scales contributions are represented by the higher-dimension operators in \mathcal{H} and by the Wilson coefficients of the operators of the nonrelativistic Hamiltonian leading to an expansion in β and α_s . On the other hand the radiation/absorption of the ultrasoft gluons by the interacting quark-antiquark pair, the effect of retardation, does not contribute in NLO and NNLO (the leading ultrasoft effects in heavy quarkonium have been recently computed in ref. [25]). Thus, the nonrelativistic Green function of eq. (1) is the basic object in NRQCD analysis of the threshold effects up to NNLO. In Sections 2.2-2.4 we relate the observables of $e^+e^- \rightarrow t\bar{t}$ annihilation and $\gamma\gamma \rightarrow t\bar{t}$ collisions in the threshold region to this Green function.

2.2 Cross sections.

We study the normalized cross sections of the top quark-antiquark pair production in e^+e^- annihilation

$$R^e(s) = \frac{\sigma(e^+e^- \rightarrow t\bar{t})}{\sigma(e^+e^- \rightarrow \mu^+\mu^-)},$$

and in $\gamma\gamma$ collisions

$$R^\gamma(s) = \frac{\sigma(\gamma\gamma \rightarrow t\bar{t})}{\sigma(e^+e^- \rightarrow \mu^+\mu^-)}$$

where the lepton cross section

$$\sigma(e^+e^- \rightarrow \mu^+\mu^-) = \frac{4\pi\alpha_{QED}^2}{3s}$$

is the standard normalization factor with α_{QED} being the fine structure constant. Here \sqrt{s} is the total energy of the colliding particles (electrons or photons) in the center of mass frame. For unpolarized initial states the following decomposition of the total cross sections is useful

$$R^e(s) = \frac{D_V}{q_t^2} R^v(s) + D_A R^a(s), \quad (2)$$

$$R^\gamma(s) = \frac{R^{++}(s) + R^{+-}(s)}{2} \quad (3)$$

where R^v (R^a) corresponds to the top quark vector (axial) coupling in e^+e^- annihilation while R^{++} (R^{+-}) corresponds to the colliding photons of the same (opposite) helicity in $\gamma\gamma$ collisions. $D_{V,A}$ are the standard combinations of electroweak coupling constants (see below), q_t is the top quark electric charge. The cross section for the polarized electron/positron initial states is discussed, e.g. in ref. [36].

Near the threshold the cross sections are determined by the imaginary part of the correlators of the nonrelativistic vector/axial quark currents which can be related to the nonrelativistic Green function and its derivatives at the origin. In NNLO the (potential) NRQCD provides one with the following representation of the cross sections

$$R^v(s) = \frac{6\pi q_t^2 N_c}{m_t^2} \left(C^v(\alpha_s) + B^v \frac{k^2}{m_t^2} \right) \text{Im}G(0, 0, k), \quad (4)$$

$$R^a(s) = \frac{4\pi N_c}{m^4} C^a(\alpha_s) \partial_{\mathbf{xy}}^2 \text{Im}G(\mathbf{x}, \mathbf{y}, k) \quad (5)$$

$$R^{++}(s) = \frac{24\pi q_t^4 N_c}{m_t^2} \left(\left(C^{++}(\alpha_s) + B^{++} \frac{k^2}{m_t^2} \right) \text{Im}G(0, 0, k) + \partial_{\mathbf{xy}}^2 \text{Im}G(\mathbf{x}, \mathbf{y}, k) \right) \quad (6)$$

$$R^{+-}(s) = \frac{32\pi q_t^4 N_c}{m^4} C^{+-}(\alpha_s) \partial_{\mathbf{xy}}^2 \text{Im}G(\mathbf{x}, \mathbf{y}, k) \quad (7)$$

where $k^2 = -m_t E$, $E = \sqrt{s} - 2m_t$ is the energy of a quark pair counted from the threshold $2m_t$. A symbolic notation $\partial_{\mathbf{xy}}^2$ is used for the operator

$$\partial_{\mathbf{xy}}^2 f(\mathbf{x}, \mathbf{y}) \equiv \sum_{i=1}^3 \partial_{x_i} (\partial_{y_i} f(\mathbf{x}, \mathbf{y})|_{y=0})|_{x=0}$$

that singles out the P partial wave of the Green function. The standard electroweak factors read

$$D_V = q_e^2 q_t^2 + 2q_e q_t v_e v_t d + (v_e^2 + a_e^2) v_t^2 d^2,$$

$$D_A = (v_e^2 + a_e^2) a_t^2 d^2,$$

$$q_e = -1, \quad v_e = -1 + 4 \sin^2 \theta_W, \quad a_e = -1,$$

$$q_t = \frac{2}{3}, \quad v_t = 1 - 8 \sin^2 \theta_W, \quad a_t = 1,$$

$$d = \frac{1}{16 \sin^2 \theta_W \cos^2 \theta_W} \frac{s}{s - M_Z^2}.$$

The coefficients $C^i(\alpha_s)$ and B^i are the parameters of NRQCD which are responsible for matching the effective and full theory cross sections in the limit of weak coupling in NNLO.

The coefficients

$$C^i(\alpha_s) = 1 + c_1^i C_F \frac{\alpha_s}{\pi} + c_2^i C_F \left(\frac{\alpha_s}{\pi} \right)^2 + \dots$$

account for the hard QCD corrections and are determined by the corresponding amplitudes with on-shell heavy quarks at rest. The numerical values of these hard coefficients in the NLO approximation have been known since long ago [37, 38, 39, 40]. They are explicitly

$$c_1^v = -4, \quad c_1^a = -2,$$

$$c_1^{++} = \frac{\pi^2}{4} - 5, \quad c_1^{+-} = -4.$$

The coefficient C^v has recently been computed in NNLO in different schemes [22, 26, 27]. Starting from NNLO the hard coefficients acquire the anomalous dimensions and the calculation of the NNLO correction requires an accurate separation of hard and soft contributions. At the same time these coefficients do not depend on the normalization point of the strong coupling constant in NNLO and one can use the different normalization points of α_s entering in the coefficients C^i (the “hard” scale μ_h) and the nonrelativistic Green function (the “soft” scale μ_s), see Section 3.1.

The coefficients B^i in eqs. (4) and (6) describe the pure relativistic corrections to the cross section which appear when the cross section is evaluated in terms of the correlator

of nonrelativistic quark currents. Because the corresponding correction first appears in the order $O(\beta^2)$ the coefficients B^i can be taken in the leading order in α_s . The coefficient B^v is related to the nonrelativistic expansion of the vector current and is known [8] to be equal to

$$B^v = \frac{4}{3}.$$

The calculation of the coefficient B^{++} necessary for the consistent description of the $\gamma\gamma$ cross section within NRQCD in NNLO is more involved because the amplitude of $\gamma\gamma \rightarrow t\bar{t}$ transition is determined by the nonrelativistic expansion of a T product of two vector currents [31, 41]. This coefficient, however, can be found by direct comparison with the relativistic expression for the cross section expanded in the velocity of the heavy quark (see Section 3.1).

For the noninteracting quarks (the Born approximation) one obtains the following results for the cross sections ($\beta = \sqrt{1 - 4m_t^2/s}$)

$$\begin{aligned} R^v(\beta) &= \frac{3}{2}q_t^2 N_c \theta(\beta^2)(\beta + O(\beta^3)), & R^a(\beta) &= N_c \theta(\beta^2)(\beta^3 + O(\beta^5)), \\ R^{++}(\beta) &= 6q_t^4 N_c \theta(\beta^2)(\beta + O(\beta^3)), & R^{+-}(\beta) &= 8q_t^4 N_c \theta(\beta^2)(\beta^3 + O(\beta^5)). \end{aligned}$$

Note that the cross sections R^v and R^{++} are saturated with the S wave contribution and are proportional to the Green function at the origin while R^a and R^{+-} parts are saturated with the P wave contribution and are proportional to the derivative of the Green function at the origin. As a consequence they are suppressed in comparison with R^v and R^{++} by factor β^2 . In the present paper we study the corrections to the total cross sections R^e and R^γ up to the NNLO of NRQCD. Thus R^a is a NNLO contribution to the total cross section R^e and only the leading contribution to R^a is important. On the contrary, the R^{+-} part can be separated from R^γ by fixing the opposite helicities of the colliding photons. This makes possible the direct study of the P wave production and, therefore, the evaluation of the corrections to R^{+-} cross section is of practical interest.

Concluding this subsection we should also mention that the electroweak corrections to the cross sections are known to the one-loop accuracy. For e^+e^- annihilation they have been

obtained in ref. [42] and for $\gamma\gamma$ collisions in ref. [43].

2.3 Forward-backward asymmetry.

The important parameter related to threshold production is a space asymmetry of the differential cross sections. This parameter gives more detailed information on the process and allows one to obtain independent experimental data for further testing the theory. The forward-backward asymmetry of the top quark production is defined as a difference of cross sections averaged over forward and backward semispheres with respect to the electron beam direction divided by the total cross section. A nonvanishing asymmetry appears in e^+e^- annihilation due to the axial coupling of the top quark to the Z -boson. The expression of this parameter for energies near the threshold is given by [5]

$$A_{FB} = \frac{E_{VA}}{D_V} \left(1 + \frac{c_1^a - c_1^v}{2} \frac{C_F \alpha_s}{\pi} \right) \Phi(k) \quad (8)$$

where

$$E_{VA} = q_e q_t a_e a_t d + 2v_e a_e v_t a_t d^2$$

is the electroweak factor. The expression for the asymmetry in eq. (8) is given in NLO and the explicit correction of order α_s is taken in the linear approximation that leads to the manifest difference of axial and vector hard coefficients in this order.

The dynamical quantity is a function

$$\Phi(k) = \frac{1}{m_t} \frac{\text{Re} \int \tilde{G}^*(p, k) \tilde{F}(p, k) p^3 dp}{\int \tilde{G}^*(p, k) \tilde{G}(p, k) p^2 dp} \quad (9)$$

that describes the overlap of the S and P partial waves. Here $\mathbf{p}\tilde{F}(p, k)$ and $\tilde{G}(p, k)$ are the Fourier transforms of $i\partial_{\mathbf{y}}G(\mathbf{x}, \mathbf{y}, k)|_{y=0}$ and $G(x, 0, k)$ correspondingly. In the Born approximation the expression for the function $\Phi(\beta)$ can be found in the explicit form and is rather simple $\Phi(\beta) = \text{Re} \beta$. It vanishes for the real values of energy below threshold.

2.4 Top quark polarization.

The longitudinal top quark polarization in the process $e^+e^- \rightarrow t\bar{t}$ averaged over the production angle reads [6, 44]

$$\langle P_L \rangle = -\frac{4}{3} \frac{D_{VA}}{D_V} \left(1 + \frac{c_1^a - c_1^v}{2} \frac{C_F \alpha_s}{\pi} \right) \Phi(k)$$

where

$$D_{VA} = q_e q_t v_e a_t d + (v_e^2 + a_e^2) v_t a_t d^2$$

and $\Phi(k)$ is given by eq. (9). This function enters also the expression for the averaged longitudinal top quark polarization in $\gamma\gamma \rightarrow t\bar{t}$ process with the same helicity colliding photons [7]

$$\langle P_L \rangle = \pm 2 \left(1 + \frac{c_1^{+-} - c_1^{++}}{2} \frac{C_F \alpha_s}{\pi} \right) \Phi(k)$$

where $+$ ($-$) correspond to the positive (negative) helicity photons.

The extension of the above expressions to the general electron/positron polarization and photon helicity and to other component of the polarization vector can be found in the literature (e.g. refs. [6, 7]).

2.5 The effects of the finite top quark width.

As has already been mentioned the sufficiently large t -quark decay width suppresses the nonperturbative effects of strong interactions at large ($\sim 1/\Lambda_{QCD}$) distances and makes the perturbation theory applicable for the description of the t -quark threshold dynamics. The near-threshold dynamics is nonrelativistic and is rather insensitive to the hard momentum details of t -quark decays. Therefore as the leading order approximation the instability of the top quark can be parameterized with the constant mass operator. The finite top quark width can then be taken into account by the direct replacement $m_t \rightarrow m_t - i\Gamma_t/2$ in the relevant argument $s - 4m_t^2$ describing the functional dependence of physical quantities near the

threshold, or $E \rightarrow E + i\Gamma_t$ [1]. This approximation accounts for the leading imaginary electroweak contribution to the leading order NRQCD Lagrangian. Since the essential features of the physical situation are caught within this approximation we neglect the electroweak effects in higher orders in the strong coupling constant and heavy quark velocity. However, in the case of P wave production and $S - P$ wave interference the above prescription is not sufficient for a proper description of the entire effect of the non-zero top quark width [2] and more thorough analysis is necessary (see Sections 3.2, 3.3).

In the context of the top quark finite lifetime we should also mention the unfactorizable corrections due to the top quark interaction with the decay products which are suppressed in the total cross sections [45] but should be taken into account as NLO contributions to the angular distribution and top quark polarization [46].

3 Nonrelativistic Green function beyond the leading order.

The basic quantity in the analysis of the threshold effects is the nonrelativistic Green function of the Schrödinger equation (1). The Green function has a standard partial wave decomposition

$$G(\mathbf{x}, \mathbf{y}, k) = \sum_{l=0}^{\infty} (2l+1)(xy)^l P_l(\mathbf{xy}/xy) G_l(x, y, k) \quad (10)$$

where $P_l(z)$ is a Legendre polynomial. The partial waves of the Green function of the pure Coulomb Schrödinger equation $G^C(\mathbf{x}, \mathbf{y}, k)$ are known explicitly

$$G_l^C(x, y, k) = \frac{m_t k}{2\pi} (2k)^{2l} e^{-k(x+y)} \sum_{m=0}^{\infty} \frac{L_m^{2l+1}(2kx) L_m^{2l+1}(2ky) m!}{(m+l+1-\nu)(m+2l+1)!} \quad (11)$$

where $\nu = \lambda/k$, $\lambda = \alpha_s C_F m_t/2$ with α_s is taken at the soft scale μ_s . $L_m^\alpha(z)$ is a Laguerre polynomial which is chosen in the form

$$L_m^\alpha(z) = \frac{e^z z^{-\alpha}}{m!} \left(\frac{d}{dz} \right)^m (e^{-z} z^{m+\alpha}).$$

We, however, need to know the nonrelativistic Green function for the NNLO Hamiltonian of the following form

$$\mathcal{H} = \mathcal{H}_C + \Delta\mathcal{H}.$$

The second term of this expression describes the corrections to the Coulomb Hamiltonian

$$\Delta\mathcal{H} = -\frac{\Delta_{\mathbf{x}}^2}{4m_t^3} + \Delta_1 V(x) + \Delta_2 V(x) + \Delta_{NA} V(x) + \Delta_{BF} V(\mathbf{x}, \partial_{\mathbf{x}}, \mathbf{S}). \quad (12)$$

The first term of the equation is the standard correction to the kinetic energy operator, $\Delta_{NA} V(x) = -C_A C_F \alpha_s^2 / (2m_t x^2)$ is the so called non-Abelian potential of quark-antiquark interaction [47] and $\Delta_{BF} V(\mathbf{x}, \partial_{\mathbf{x}}, \mathbf{S})$ is a standard Breit-Fermi potential known since long ago (only the overall color factor C_F is new). The Breit-Fermi potential contains the quark spin operator \mathbf{S} , *e.g.* [48]. In NNLO the cross section R^v is saturated by the final state configuration of $t\bar{t}$ pair with $l = 0, S = 1$ while R^{++} cross section is saturated by $l = 0, S = 0$ configuration. The Breit-Fermi potential takes the following form when considered on the $l = 0$ states

$$\Delta_{BF} V(x) = \frac{C_F \alpha_s}{x} \frac{\Delta_{\mathbf{x}}}{m_t^2} + A^i \frac{C_F \alpha_s \pi}{m_t^2} \delta(\mathbf{x})$$

where $A^v = 11/3$ corresponds to the spin one final state of $e^+e^- \rightarrow t\bar{t}$ production and $A^{++} = 1$ corresponds to the spin zero final state of $\gamma\gamma \rightarrow t\bar{t}$ production.

The terms $\Delta_i V$ ($i = 1, 2$) represent the first and second order perturbative QCD corrections to the Coulomb potential [49, 50]

$$\begin{aligned} \Delta_1 V(x) &= \frac{\alpha_s}{4\pi} V_C(x) (C_0^1 + C_1^1 \ln(x\mu_s)), \\ \Delta_2 V(x) &= \left(\frac{\alpha_s}{4\pi}\right)^2 V_C(x) (C_0^2 + C_1^2 \ln(x\mu_s) + C_2^2 \ln^2(x\mu_s)) \end{aligned}$$

where

$$\begin{aligned} C_0^1 &= a_1 + 2\beta_0 \gamma_E, & C_1^1 &= 2\beta_0, \\ C_0^2 &= \left(\frac{\pi^2}{3} + 4\gamma_E^2\right) \beta_0^2 + 2(\beta_1 + 2\beta_0 a_1) \gamma_E + a_2, \end{aligned}$$

$$\begin{aligned}
C_1^2 &= 2(\beta_1 + 2\beta_0 a_1) + 8\beta_0^2 \gamma_E, & C_2^2 &= 4\beta_0^2, \\
a_1 &= \frac{31}{9}C_A - \frac{20}{9}T_F n_f, \\
a_2 &= \left(\frac{4343}{162} + 4\pi^2 - \frac{\pi^4}{4} + \frac{22}{3}\zeta(3) \right) C_A^2 - \left(\frac{1798}{81} + \frac{56}{3}\zeta(3) \right) C_A T_F n_f \\
&\quad - \left(\frac{55}{3} - 16\zeta(3) \right) C_F T_F n_f + \left(\frac{20}{9}T_F n_f \right)^2, \\
\beta_1 &= \frac{34}{3}C_A^2 - \frac{20}{3}C_A T_F n_f - 4C_F T_F n_f.
\end{aligned}$$

Here α_s is defined in $\overline{\text{MS}}$ renormalization scheme. The invariants of the color symmetry $SU(3)$ group have the following numerical values for QCD: $C_A = 3$, $C_F = 4/3$, $T_F = 1/2$, $n_f = 5$ is the number of light quark flavors, $\beta_0 = 11C_A/3 - 4T_F n_f/3$ is the first β -function coefficient, $\gamma_E = 0.577216\dots$ is the Euler constant and $\zeta(z)$ is the Riemann ζ -function. The solution to eq. (1) with the Hamiltonian (12) can be found within the standard nonrelativistic perturbation theory around the Coulomb Green function as a leading order approximation

$$\begin{aligned}
G(\mathbf{x}, \mathbf{y}, k) &= G_C(\mathbf{x}, \mathbf{y}, k) + \Delta G(\mathbf{x}, \mathbf{y}, k), \\
\Delta G(\mathbf{x}, \mathbf{y}, k) &= - \int G_C(\mathbf{x}, \mathbf{z}, k) \Delta \mathcal{H} G_C(\mathbf{z}, \mathbf{y}, k) d\mathbf{z} + \dots
\end{aligned} \tag{13}$$

In the previous section the threshold effects in the basic observables were reduced to three universal functions: the Green function at the origin which is saturated by the S wave contribution, the derivative of the Green function at the origin which is saturated by the P wave contribution and the function $\Phi(k)$ which describes the $S - P$ wave interference. These functions are analyzed in detail in Sections 3.1-3.3

3.1 S wave production.

Only the $l = 0$ component of the Green function (10) contributes to its value at the origin

$$G(0, 0, k) = G_0(0, 0, k).$$

The explicit expression for the Coulomb part of the Green function has the form

$$G_0^C(x, 0, k)|_{x \rightarrow 0} = \frac{m_t}{4\pi} \left(\frac{1}{x} - 2\lambda \ln(2x\mu_f) - 2\lambda \left(\frac{k}{2\lambda} + \ln \left(\frac{k}{\mu_f} \right) + 2\gamma_E - 1 + \Psi_1(1 - \nu) \right) \right) \quad (14)$$

where $\Psi_n(z) = d^n \ln \Gamma(z) / dz^n$ and $\Gamma(z)$ is the Euler Γ -function. The energy independent finite part of this expression is chosen for later convenience. Eq. (14) can be most easily obtained from the general expression for the Coulomb partial waves

$$G_l^C(x, 0, k) = \frac{m_t k}{2\pi} (2k)^{2l} e^{-kx} \Gamma(l + 1 - \nu) U(l + 1 - \nu, 2l + 2, 2kx) \quad (15)$$

where $U(a, b, z)$ is the confluent hypergeometric function. In the short distance limit $x \rightarrow 0$ the Coulomb Green function $G^C(\mathbf{x}, 0, k) = G_0^C(x, 0, k)$ has $1/x$ and $\ln(x)$ divergent terms. These terms, however, are energy independent and do not contribute to the cross section. Hence these terms can be subtracted without affecting any physical results. The quantity μ_f in eq. (14) is an auxiliary parameter, the factorization scale, which drops out from the physical observables.

The NLO correction $\Delta_1 G$ to eq. (14) due to the first iteration of $\Delta_1 V$ term of the QCD potential has been found in ref. [18] where the simple and efficient framework for computation of higher orders was formulated. The result of the evaluation of the NLO correction is

$$\begin{aligned} \Delta_1 G_0(0, 0, k) = & \frac{\alpha_s \beta_0}{2\pi} \frac{\lambda m_t}{2\pi} \left(\sum_{m=0}^{\infty} F(m)^2 (m+1) (L_1(k) + \Psi_1(m+2)) - 2 \sum_{m=1}^{\infty} \sum_{n=0}^{m-1} F(m) \right. \\ & \left. \times F(n) \frac{n+1}{m-n} + 2 \sum_{m=0}^{\infty} F(m) (L_1(k) - 2\gamma_E - \Psi_1(m+1)) - \gamma_E L_1(k) + \frac{1}{2} L_1(k)^2 \right) \end{aligned}$$

where

$$L_1(k) = \ln \left(\frac{\mu_s e^{C_0^1/C_1^1}}{2k} \right)$$

and

$$F(m) = \frac{\nu}{(m+1)(m+1-\nu)}.$$

The NNLO correction $\Delta_2^{(2)}G$ due to Δ_2V part of the potential and the correction $\Delta_2^{(1)}G$ due to the second iteration of Δ_1V part of the correction to the Coulomb static potential have been obtained in refs. [18, 19]. While the technique is rather straightforward the results of the calculations are cumbersome and explicit formulae are relegated to Appendix A.

The method of calculation of the correction to the Green function at the origin due to logarithmic terms in the potential is described in details in ref. [21]. It is based on the representation of the Coulomb Green function as an expansion over the Laguerre polynomials (11). This representation is very close to the standard physical expansion over the eigenfunctions that makes the technique transparent and easily interpretable in physical terms. It is equally suitable for any partial wave contribution as has been shown in ref. [31] where results for the P wave production were found. The results for the S wave part of the corrections were reproduced within a different technical framework based on an integral representation of the Coulomb Green function in ref. [20].

The corrections to the Coulomb Green function at the origin due to Δ^2 , V_{NA} and V_{BF} terms have been presented in [26, 27]. They are of the following explicit form

$$\begin{aligned} \Delta_{\Delta^2, NA, BF}G = & \frac{m_t}{4\pi} \frac{k^2}{m_t^2} \left(\frac{5}{8}k + 4\lambda \left(\ln \left(\frac{k}{\mu_f} \right) + \gamma_E + \Psi_1(1 - \nu) \right) - \frac{11}{8}C_F\alpha_s\nu\Psi_2(1 - \nu) \right) \\ & + \pi \frac{C_F\alpha_s}{m_t^2} \left(5 - A^i + 2\frac{C_A}{C_F} \right) G_C(0, 0, k)^2. \end{aligned} \quad (16)$$

In the course of evaluation of this correction to the nonrelativistic Green function one encounters the ultraviolet divergence in the imaginary part of the Green function contained in the last term of eq. (16). This divergence is related to the singular behavior of the Coulomb Green function at the origin. The particular form of this divergence depends on the regularization procedure. The divergence appears in the process of scale separation and is a consequence of the fact that the nonrelativistic approximation is not adequate for the description of the short distance effects. The hard coefficient $C^{v,++}$ computed within the same regularization procedure as the Green function itself must have the infrared singular term

which exactly cancels the one appearing in the Green function. The hard coefficient can be evaluated by matching the effective and full theory cross sections in the weak coupling limit [17, 26] or by an explicit splitting of the hard and soft contributions using, for example, the scale factorization in dimensional regularization [22, 34, 35]. Let us consider the cancelation of the divergences and determination of the hard coefficient in the matching scheme. The natural regularization for the analysis of the hard part of the corrections is the dimensional one [32, 33]. In $4 - 2\varepsilon$ dimensions the infrared divergence of the hard contribution in NNLO has the form of the first order pole in ε . The Coulomb Green function at the origin in eq. (16) can be regularized in the same way. The dimensionally regularized Coulomb Green function at the origin can be defined as follows (see Appendix B)

$$G_C^{d.r.}(0, 0, k) = -\frac{m_t}{4\pi} \left(k + 2\lambda \left(-\frac{1}{2\varepsilon} + \ln \left(\frac{k}{\mu_f} \right) + \gamma_E + \Psi_1(1 - \nu) \right) \right) + O(\varepsilon). \quad (17)$$

Note that the Green function regularized in this way differs from that which has been obtained in ref. [35] within another scheme of dimensional regularization. In contrast to eq. (14) in eq. (17) there is no divergence in the Born approximation. The Green function in this approximation is a nonrelativistic free propagator and is proportional to k . The first order pole in ε appears only in the first order in α_s . The $O(\alpha^2)$ singular $1/\varepsilon$ term in the imaginary part of eq. (16) is proportional to $\text{Im}(G_C(0, 0, k))$ and, therefore, can be absorbed by the redefinition of the hard coefficient $C^{v,++}$. For the Green function this redefinition results in the substitution $G_C^{d.r.}(0, 0, k) \rightarrow G_C^s(0, 0, k)$ in eq. (16) where the “subtracted” Green function reads

$$G_C^s(0, 0, k) = G_C^{d.r.}(0, 0, k) - \frac{m_t \lambda}{4\pi} \frac{1}{\varepsilon}. \quad (18)$$

Within the redefined hard coefficient the $O(\alpha^2)$ “ultraviolet” $1/\varepsilon$ term stemming from the corrections to the Green function eq. (16) exactly cancels the $O(\alpha^2)$ “infrared” $1/\varepsilon$ term of the hard part of the corrections regularized in the same way. Then the (finite) coefficient $C^{v,++}$ can be found directly by matching the effective theory expression for the cross sections and the result of perturbative QCD calculation of the spectral density in the formal limit

$\alpha_s \ll \beta \ll 1$ up to the order α_s^2 for $\mu_h = \mu_s$. Eqs. (2, 3) in the matching limit take the form

$$\begin{aligned}
R^v &= \frac{3}{2} N_c q_t^2 \beta \left((1 + (1 - B^v) \beta^2) + C_F \frac{\alpha_s}{\pi} \left(\frac{\pi^2}{2} \frac{1}{\beta} + c_1^v + \frac{\pi^2}{3} \beta \right) \right. \\
&+ C_F \left(\frac{\alpha_s}{\pi} \right)^2 \left(C_F \frac{\pi^4}{12} \frac{1}{\beta^2} + \pi^2 \left(C_F \frac{c_1^v}{2} + \frac{1}{8} \left(-C_1^1 \ln \left(\frac{2\beta m_t}{\mu_s} \right) + C_0^1 - 2\beta_0 \gamma_E \right) \right) \right) \frac{1}{\beta} \\
&\left. + C_F \frac{5\pi^4}{36} + c_2^v - C_F \pi^2 \left(\frac{5 - A^v}{2} + \frac{C_A}{C_F} \right) \ln \left(\frac{\beta m_t}{\mu_f} \right) \right), \tag{19}
\end{aligned}$$

$$\begin{aligned}
R^{++} &= 6 N_c q_t^4 \beta \left((1 + (1 - B^{++}) \beta^2) + C_F \frac{\alpha_s}{\pi} \left(\frac{\pi^2}{2} \frac{1}{\beta} + c_1^{++} + \frac{\pi^2}{3} \beta \right) \right. \\
&+ C_F \left(\frac{\alpha_s}{\pi} \right)^2 \left(C_F \frac{\pi^4}{12} \frac{1}{\beta^2} + \pi^2 \left(C_F \frac{c_1^{++}}{2} + \frac{1}{8} \left(-C_1^1 \ln \left(\frac{2\beta m_t}{\mu_s} \right) + C_0^1 - 2\beta_0 \gamma_E \right) \right) \right) \frac{1}{\beta} \\
&\left. + C_F \frac{5\pi^4}{36} + c_2^{++} - C_F \pi^2 \left(\frac{5 - A^{++}}{2} + \frac{C_A}{C_F} \right) \ln \left(\frac{\beta m_t}{\mu_f} \right) \right) + R_P^{++} \tag{20}
\end{aligned}$$

where the terms of the relative order $O(\beta^2)$ are kept. In eq. (20) the P wave contribution

$$R_P^{++} = 6 N_c q_t^4 \beta^3 + \dots$$

is due to the derivative term in eq. (6) to be discussed. By comparing eq. (19) with the NNLO QCD result for the cross section R^v expanded in the velocity of the heavy quark near the threshold [32, 51] one finds

$$c_2^v = \tilde{c}_2^v - c_1^v \frac{\beta_0}{2} \ln \left(\frac{m_t}{\mu_h} \right) + \pi^2 \left(\frac{2}{3} C_F + C_A \right) \ln \left(\frac{m_t}{\mu_f} \right), \tag{21}$$

where the coefficient \tilde{c}_2^v has been obtained in refs. [26, 27]

$$\begin{aligned}
\tilde{c}_2^v &= \left(\frac{39}{4} - \zeta(3) + \frac{4\pi^2}{3} \ln 2 - \frac{35\pi^2}{18} \right) C_F - \left(\frac{151}{36} + \frac{13}{2} \zeta(3) + \frac{8\pi^2}{3} \ln 2 - \frac{179\pi^2}{72} \right) C_A \\
&+ \left(\frac{44}{9} - \frac{4\pi^2}{9} + \frac{11}{9} n_f \right) T_F.
\end{aligned}$$

The first logarithm in eq. (21) is determined by the renormalization group running of the strong coupling constant in the hard momentum regime and is proportional to the first coefficient of the β function. Thus, both the hard coefficient and the imaginary part of

the Green function do not depend on the normalization point of α_s in the fixed order of perturbation theory so one can use different scales for α_s in these quantities. The second logarithm corresponds to the anomalous dimension of the hard coefficient and precisely cancels the factorization scale dependence of the Green function due to eq. (16) making the total result independent of the factorization scale. Note that the use of different hard and soft normalization scales leads to the incomplete cancelation of the factorization scale dependence which, however, is the higher order ($O(\alpha_s^3)$) effect.

As it has been mentioned above one can bypass the direct matching by the consistent use of the same subtraction scheme within dimensional regularization for both hard coefficient and Green function. Then matching is automatic [14, 34, 35]. In this approach the hard coefficient is completely determined by the hard renormalization coefficient of the nonrelativistic vector current [22]. However, in order to compute the corrections to the Green function in this case one has to define accurately the Breit-Fermi Hamiltonian and the Green function in $3 - 2\varepsilon$ dimensions [22, 35] (in our analysis we use three dimensional Breit-Fermi Hamiltonian and direct regularization of the Green function therefore the matching is necessary in order to fix the constant relating the two regularization schemes).

The NNLO analysis of the R^{++} cross section is still absent and the constant in the hard coefficient is unknown. The logarithmic part of the NNLO contribution to $C^{++}(\alpha_s)$ reads

$$c_2^{++} = \tilde{c}_2^{++} - c_1^{++} \frac{\beta_0}{2} \ln \left(\frac{m_t}{\mu_h} \right) + \pi^2 (2C_F + C_A) \ln \left(\frac{m_t}{\mu_f} \right) \quad (22)$$

where \tilde{c}_2^{++} is a constant to be determined. The relativistic correction to this cross section, however, can be extracted from the calculations presented earlier in the literature. Comparing the known result [52]

$$R^{++}(\beta) = 6q_t^4 N_c \beta \left(1 + \frac{2}{3} \beta^2 + O(\beta^4) \right) \quad (23)$$

with our expressions from eqs. (20, 23) we find

$$B^{++} = \frac{4}{3}.$$

The Green function at the origin can be written in the form which includes only single poles in the energy variable. This form seems to be natural for a Green function of the nonrelativistic Schrödinger equation

$$G(0, 0, E) = \sum_{m=0}^{\infty} \frac{|\psi_{0m}(0)|^2}{E_{0m} - E} + \frac{1}{\pi} \int_0^{\infty} \frac{|\psi_{0E'}(0)|^2}{E' - E} dE' \quad (24)$$

where $\psi_{0m,E'}(0)$ is the wave function at the origin, the sum goes over the bound states and the integral goes over the states of a continuous part of the spectrum. In this way the corrections to the Green function stemming from the discrete part of the spectrum reduce to corrections to Coulomb bound state energy levels

$$E_{0m} = E_{0m}^C (1 + \Delta_1 E_{0m} + \Delta_2 E_{0m})$$

and to the values of Coulomb bound state wave functions at the origin

$$|\psi_{0m}(0)|^2 = |\psi_{0m}^C(0)|^2 (1 + \Delta_1 \psi_{0m}^2 + \Delta_2 \psi_{0m}^2)$$

where

$$E_{0m}^C = -\frac{\lambda^2}{m_t(m+1)^2}, \quad |\psi_{0m}^C(0)|^2 = \frac{\lambda^3}{\pi(m+1)^3},$$

$$\Delta_2 E_{0m} = \Delta_{\Delta^2, NA, BF} E_{0m} + \Delta_2^{(2)} E_{0m} + \Delta_2^{(1)} E_{0m},$$

$$\Delta_2 \psi_{0m}^2 = \Delta_{k^2} \psi_{0m}^2 + \Delta_{\Delta^2, NA, BF} \psi_{0m}^2 + \Delta_2^{(2)} \psi_{0m}^2 + \Delta_2^{(1)} \psi_{0m}^2$$

and $\Delta_{k^2} \psi_{0m}^2$ is the correction due to relativistic corrections parameterized by the coefficients B^i which we include into the definition of the wave function.

In NLO an explicit analytical expression for the corrections to the bound state parameters has the form [20, 21, 53]

$$\Delta_1 E_{0m} = \frac{\alpha_s \beta_0}{\pi} (\bar{L}_1(m) + \Psi_1(m+2)),$$

$$\Delta_1 \psi_{0m}^2 = \frac{\alpha_s \beta_0}{2\pi} \left(3\bar{L}_1(m) + \Psi_1(m+2) - 2(m+1)\Psi_2(m+1) - 1 - 2\gamma_E + \frac{2}{m+1} \right)$$

where $\bar{L}_1(m) = L_1(\lambda/(m+1))$. The expressions of the NNLO corrections to the energy levels [20, 21, 53] and wave functions at the origin [20, 21] are rather cumbersome and given in Appendix C, D.

The continuum contributions in eq. (24) can be directly found by subtracting the discrete part of these equations expanded around the Coulomb approximation up to NNLO

$$\sum_{m=0}^{\infty} \frac{|\psi_{0m}^C(0)|^2}{E_{0m}^C - E} \left(1 + \Delta_1 \psi_{0m}^2 + \Delta_2 \psi_{0m}^2 + \frac{(1 + \Delta_1 \psi_{0m}^2) \Delta_1 E_{0m} + \Delta_2 E_{0m}}{1 - E/E_{0m}^C} + \frac{\Delta_1 E_{0m}^2}{(1 - E/E_{0m}^C)^2} \right)$$

from the result obtained within the nonrelativistic perturbation theory for the Green function at the origin (13) multiplied by $(1 - B^i E/m_t)$. This procedure removes the double and triple poles from eq. (13) and leaves only the single poles in the expression for the Green function (24).

An important consequence of the relatively large top quark width is that the most of Coulomb resonances are smoothed out. The numerical analysis shows that only the ground state resonance in the cross sections is distinguishable. Its separation from others is not completely covered by the infrared cutoff provided by the top quark width. Indeed, using the pure Coulomb formulas for estimates within the order of magnitude we find

$$|E_{00}^C - E_{01}^C| = \frac{3\lambda^2}{4m_t} \approx 0.6 \text{ GeV}$$

to be compared with the top quark width $\Gamma_t = 1.43 \text{ GeV}$. The second spacing between radial excitations for the $l = 0$ partial wave and the first spacing for the $l = 1$ partial wave are, however, much smaller

$$|E_{01}^C - E_{02}^C| = |E_{10}^C - E_{11}^C| = \frac{5}{36} \frac{\lambda^2}{m_t} \approx 0.11 \text{ GeV}.$$

Therefore the contributions of higher resonances are completely smeared out with the top quark width.

In the limit of vanishing top quark width the NNLO approximation for the energy of the first resonance in e^+e^- annihilation reads

$$\begin{aligned}
E_{00}^v = & -\frac{\lambda^2}{m_t} \left(1 + \frac{\alpha_s}{4\pi} 2C_1^1 (L_1(\lambda) + 1 - \gamma_E) + \left(\frac{\alpha_s}{4\pi} \right)^2 \left(2C_1^2 (L_2(\lambda) + 1 - \gamma_E) \right. \right. \\
& + (C_1^1)^2 \left((L_1(\lambda) - \gamma_E)^2 + 1 - \frac{\pi^2}{3} - \Psi_3(1) \right) + 2C_2^2 \left((L(\lambda) + 1 - \gamma_E)^2 - 1 + \frac{\pi^2}{6} \right) \\
& \left. \left. + C_F^2 \alpha_s^2 \left(\frac{C_A}{C_F} + \frac{1}{48} \right) \right) \right) \quad (25)
\end{aligned}$$

where

$$L(\lambda) = \ln \left(\frac{\mu_s}{2\lambda} \right), \quad L_2(\lambda) = \ln \left(\frac{\mu_s e^{C_0^2/C_1^2}}{2\lambda} \right).$$

This value is related to the energy of the resonance of the top quark production in $\gamma\gamma$ collision by the hyperfine splitting

$$E_{00}^v - E_{00}^{++} = \frac{4}{3} \frac{\lambda^2}{m_t} C_F^2 \alpha_s^2.$$

The convergence of the perturbation theory series (25) is not fast. For some typical values of the soft normalization scale the series for the resonance energy reads

$$\begin{aligned}
E_{00}^v &= E_{00}^{LO} (1 + 0.36 + 0.30), & \mu_s &= 25 \text{ GeV}, \\
E_{00}^v &= E_{00}^{LO} (1 + 0.58 + 0.38), & \mu_s &= 50 \text{ GeV}, \\
E_{00}^v &= E_{00}^{LO} (1 + 0.68 + 0.45), & \mu_s &= 75 \text{ GeV}, \\
E_{00}^v &= E_{00}^{LO} (1 + 0.74 + 0.50), & \mu_s &= 100 \text{ GeV}.
\end{aligned} \quad (26)$$

The poor convergence of the series for the resonance energy can be assigned to high infrared sensitivity of the pole mass (see, for example, [54]). The convergence can be manifestly improved by removing the pole mass from the theoretical expressions in favor of some less infrared sensitive mass parameter, for example, the short-distance [20], potential-subtracted [22] or $1S$ mass [24]. Note that in a finite order of the expansion all the mass definitions are perturbatively equivalent. The infrared safe mass parameters, however, are “closer” to the

physical observables since in contrast to the pole mass the corresponding perturbative series are supposed to be better convergent (less divergent).

Due to the finite top quark width the location of the peak (maximum) of the cross section is not given only by the position of the ground state resonance but is also affected by the contribution of the higher (smeared out) resonances and the continuum contribution. Due to this effect the absolute value of the NNLO peak energy (25) counted from the threshold is less than the absolute value of the energy of the ground state resonance $E_{00}^{v,++}$ by about 200 MeV *i.e.* $\sim 7\%$. This shift is essentially smaller than the one related to the perturbative QCD corrections to Coulomb values but considerably larger than the leading nonperturbative contribution due to the gluon condensate [55] which is suppressed parametrically as $(\Lambda_{QCD}/\lambda)^4 < 1\%$.

3.2 P wave production.

The derivative of the Green function at the origin is saturated with its $l = 1$ component and explicitly given by the relation

$$\partial_{\mathbf{xy}}^2 G(\mathbf{x}, \mathbf{y}, k) = 9G_1(0, 0, k).$$

For the Coulomb Green function from eq. (15) we obtain the closed formula for the partial wave $l = 1$ Green function at the small space separation of particle

$$\begin{aligned} G_1^C(x, 0, k)|_{x \rightarrow 0} = & \frac{m_t}{36\pi} \left(\frac{3}{x^3} + \frac{3\lambda}{x^2} + \frac{6\lambda^2 - 3k^2}{2x} + 2\lambda(k^2 - \lambda^2) \ln(2x\tilde{\mu}_f) \right. \\ & \left. + \lambda \left(2(k^2 - \lambda^2) \left(\frac{k}{2\lambda} + \ln \left(\frac{k}{\tilde{\mu}_f} \right) + 2\gamma_E - \frac{11}{6} + \Psi_1(1 - \nu) \right) + \frac{k^2}{2} \right) \right) \end{aligned} \quad (27)$$

where $\tilde{\mu}_f$ is the analog of the parameter μ_f for the $l = 0$ partial wave. In the short distance limit $x \rightarrow 0$ the derivative of the Coulomb Green function (or the partial wave with $l = 1$) has $1/x^n$ ($n = 1, 2, 3$) and $\ln(x)$ singularities. In contrast to the case of the S wave production, the value at the origin for the P wave partial Green function contains divergent terms

that explicitly depends on the energy (or wave vector) k . However, these terms do not contribute to the cross section for the vanishing top quark width $\Gamma_t = 0$ because they have no discontinuity across the physical cut in the complex plane of the energy variable in the approximation of top quark zero width. The case of the non-zero top quark width requires to perform a more detailed analysis given below.

The correction to the $l = 1$ partial wave at the origin due to the first iteration of $\Delta_1 V$ term of the QCD potential has been found in ref. [31]

$$\begin{aligned} \Delta_1 G_1(0, 0, k) &= \frac{\alpha_s \beta_0}{2\pi} \frac{\lambda m_t k^2}{18\pi} \left(\sum_{m=0}^{\infty} \tilde{F}(m)^2 (m+1)(m+2)(m+3) (L_1(k) + \Psi_1(m+4)) \right. \\ &- 2 \sum_{m=1}^{\infty} \sum_{n=0}^{m-1} \tilde{F}(m) \tilde{F}(n) \frac{(n+1)(n+2)(n+3)}{m-n} + 2 \sum_{m=0}^{\infty} \tilde{F}(m) \left(2\tilde{J}_0(m) + (m+1)(m+2)L_1(k) \right. \\ &\left. \left. + (1+\nu)(\tilde{J}_1(m) + (m+1)L_1(k)) + \frac{\nu(\nu+1)}{2}(\tilde{J}_2(m) + 2L_1(k)) \right) + \tilde{I}(k) \right) \end{aligned}$$

where

$$\begin{aligned} \tilde{F}(m) &= \frac{\nu(\nu^2 - 1)}{(m+2-\nu)(m+1)(m+2)(m+3)} \\ \tilde{J}_0(m) &= -2\Psi_1(m+1) - 4\gamma_E + 3, \\ \tilde{J}_1(m) &= (m+1)(-\Psi_1(m+2) - 2\gamma_E + 2), \\ \tilde{J}_2(m) &= \frac{(m+1)(m+2)}{2} \left(-\Psi_1(m+3) - 2\gamma_E + \frac{3}{2} \right), \\ \tilde{I}(k) &= -\frac{(\gamma_E - 1)^2}{2} - \frac{\pi^2}{12} - (4 - 3\gamma_E)\nu + \frac{1 - 9\gamma_E + 6\gamma_E^2 + \pi^2}{4}\nu^2 + \frac{1 - 3\gamma_E}{2}\nu^3 + \frac{1 - \gamma_E}{4}\nu^4 \\ &+ \left(\gamma_E - 1 - 3\nu + \frac{9 - 12\gamma_E}{4}\nu^2 + \frac{3}{2}\nu^3 + \frac{1}{4}\nu^4 \right) L_1(k) + \left(-\frac{1}{2} + \frac{3}{2}\nu^2 \right) L_1(k)^2 \end{aligned}$$

For the derivative of the Green function at the origin (or for the $l = 1$ partial wave) the analog of eq. (24) reads

$$\partial_{\mathbf{x}\mathbf{y}}^2 G(\mathbf{x}, \mathbf{y}, E) = \sum_{m=0}^{\infty} \frac{|\psi'_{1m}(0)|^2}{E_{1m} - E - i0} + \frac{1}{\pi} \int_0^{\infty} \frac{|\psi'_{1E'}(0)|^2}{E' - E - i0} dE'$$

where, symbolically,

$$|\psi'_{1m,E'}(0)|^2 = \partial_{\mathbf{x}} \psi_{m,E'}^*(\mathbf{x}) \partial_{\mathbf{y}} \psi_{m,E'}(\mathbf{y})|_{x,y=0}.$$

Here E_{1m} is the $l = 1$ bound state energy. In NLO approximation these quantities read [31]

$$E_{1m} = -\frac{\lambda^2}{m_t(m+2)^2} \left(1 + \frac{\alpha_s}{4\pi} 2C_1^1 \left(\bar{L}_1(m+1) + \Psi_1(m+4) \right) \right),$$

and

$$|\psi'_{1m}(0)|^2 = \frac{\lambda^5 (m+1)(m+3)}{\pi (m+2)^5} \left(1 + \frac{\alpha_s}{4\pi} C_1^1 \left(5\bar{L}_1(m+1) + 5\Psi_1(m+4) - \frac{\pi^2}{3}(m+2) - 1 \right. \right. \\ \left. \left. + 2 \sum_{n=0}^{m-1} \frac{(n+1)(n+2)(n+3)}{(m+1)(m+3)(m-n)^2} \right) \right).$$

The continuum contribution is obtained in the same way as it was done in the previous section for the S wave production.

In the case of P wave production the simple shift $E \rightarrow E + i\Gamma$ in the nonrelativistic approximation is not sufficient to describe properly the entire effect of the non-zero top quark width [2]. Indeed, eq. (27) in the limit $x \rightarrow 0$ with the nonvanishing width has the divergent imaginary part with the leading power singularity $\sim \Gamma_t/x$ related to the free Green function singularity and the logarithmic singularity $\sim \Gamma_t \alpha_s \ln(x)$ produced by the one Coulomb gluon exchange. The presence of these singularities clearly indicates that the coefficient of the constant term linear in Γ_t gets a contribution from the large momentum region and cannot be obtained within the pure nonrelativistic approximation. Like the hard coefficients it should be computed in relativistic theory. Parametrically this contribution is not suppressed in comparison to the pure nonrelativistic contribution in the threshold region. At $E = 0$, for example, the ratio between the relativistic (proportional to Γ_t) and nonrelativistic (Coulomb) contributions is of order $\frac{\Gamma_t}{\alpha_s^2 m_t} \sim 1$. Since we are interested in the NLO corrections the $O(\Gamma_t \alpha_s)$ term also has to be taken into account. By construction, the nonrelativistic effective theory has to reproduce the perturbation theory predictions in the formal matching limit $\alpha_s, \beta \ll \Gamma_t/m_t \ll 1$ where both effective theory and perturbation theory descriptions are valid. Thus one has to compute $O(\Gamma_t)$ and $O(\Gamma_t \alpha_s)$ terms within the relativistic perturbation theory and then to fix the parameters of the effective nonrelativistic

theory so that it reproduces the perturbative results in the matching limit. Within the relativistic perturbation theory the relevant contributions can be obtained by inserting the complex momentum-dependent mass operator into the top quark propagator at $\beta = 0$ (only the leading terms in Γ_t/m_t should be kept). In the leading order in α_s this procedure has been done in refs. [2]. The result reads

$$G_1^C(0, 0, k)|_{\Gamma_t} = \frac{m_t^3}{36\pi} g_1 \Gamma_t$$

where g_1 is a coefficient coming from the relativistic treatment with numerical value $g_1 = 0.185\dots$ For the term of the order $O(\Gamma_t\alpha_s)$ the necessary calculation has been performed in ref. [31]. It has been shown that the proper relativistic analysis leads to fixing the auxiliary parameter of eq. (27) $\tilde{\mu}_f = g_2 m_t$ where g_2 is the coefficient coming from the relativistic treatment. Its numerical value is $g_2 = 0.13\dots$

Here we should note also the problem of the previous numerical analysis of the P wave contribution [28]. While solving the Schrödinger equation (1) numerically for the finite top quark width one has to introduce an explicit ultraviolet cutoff for the nonrelativistic expressions divergent in the large momentum region. To get rid of the cutoff dependence one has to compute the hard contribution within the relativistic approximation using the similar prescription for the infrared cutoff. This, however, has not been done and as a consequence the $O(\Gamma_t)$ and $O(\Gamma_t\alpha_s)$ contributions to the cross section were not determined within the numerical framework of ref. [28]². On the other hand the total $O(\Gamma_t)$ contribution to the cross section is numerically small in comparison with that of the regular completely nonrelativistic terms of eq. (27) which saturate the total result for the energies not far below the threshold.

²Recently the $O(\Gamma_t)$ contribution has been estimated within the numerical approach [30] by using the physical (relativistic) phase space for the unstable top quark to regularize the divergence of the nonrelativistic approximation.

3.3 $S - P$ interference.

In the zero width approximation the function (9) allows for the following decomposition

$$\Phi(E) = \Phi_{pol}(E) + \Phi_{con}(E)$$

where Φ_{con} and Φ_{pol} are the continuum and bound state poles contributions correspondingly. This is known [7, 44] that the continuum contribution is not affected by the Coulomb effects and above the threshold one has the Born approximation result

$$\Phi_{con}^C(E) = \text{Re} \sqrt{\frac{E}{m_t}}$$

even for the Coulomb Green function in eq. (9). Below the threshold in the Coulomb approximation one gets

$$\Phi_{pol}^C(E) = \left(\sum_{m=0}^{\infty} \frac{\phi_m^C}{(E_{1m}^C - E)^2} \right) \left(\sum_{m=0}^{\infty} \frac{|\psi_m(0)|^2}{(E_{0m}^C - E)^2} \right)^{-1} \quad (28)$$

where the quantities

$$\phi_m^C = \frac{\lambda^4}{m_t \pi} \frac{(m+1)(m+3)}{(m+2)^5}$$

measure the overlap of the S and P wave functions. Note that in the zero width limit the function Φ_{pol}^C does not vanish due to the Coulomb degeneration of the energy levels with different l : $E_{0m+1}^C = E_{1m}^C$. It was pointed in ref. [44] that the continuum contribution gets no soft corrections. Thus in NLO for a finite top quark width we have the simple result

$$\Phi_{con}(E) = \text{Re} \sqrt{\frac{E + i\Gamma_t}{m_t}}.$$

The corrections to the pole contribution are less trivial. They can be computed using the powerful technique developed in refs. [18, 21, 31]. The result reads

$$\Phi_{pol}(E) = \text{Re} \left(\sum_{m=0}^{\infty} \frac{\phi_m}{(E_{0(m+1)} - E + i\Gamma_t)(E_{1m} - E - i\Gamma_t)} \right) \left(\sum_{m=0}^{\infty} \frac{|\psi_m(0)|^2}{(E_{0m} - E)^2 + \Gamma_t^2} \right)^{-1} \quad (29)$$

where

$$\phi_m = \phi_m^C \left(1 + \frac{\alpha_s \beta_0}{\pi} \left(4L(m+1) + 4\Psi(m+4) + \frac{m}{m+3} - 2 - \frac{\pi}{6}(m+2) \right) \right)$$

$$+ \sum_{n=0}^{m-1} \frac{(n+1)(n+2)(n+3)}{(m+1)(m+3)(m-n)^2} \Bigg)$$

In eq. (29) we keep the finite top quark width to get a nonvanishing result since the Coulomb degeneration is lifted by the logarithmic corrections to the potential. Strictly speaking, our approach is valid only if the level splitting $E_{0m+1} - E_{1m}$ is much smaller than the top quark width (which is realized for the actual values of these quantities). For $E_{0m+1} - E_{1m} > \Gamma_t$ the nonrelativistic analysis is not applicable for the $S - P$ interference below the threshold because the double poles of eq. (28) disappear and the nonrelativistic contribution is not enhanced in comparison to the relativistic one in this case.

Note that for the finite top quark width the interference of the free $l = 0$ and $l = 1$ partial waves results in the logarithmically divergent $O(\Gamma_t)$ term in the numerator of eq. (9) (this term does not include the factor Γ_t explicitly but it is suppressed in comparison to the leading term which is proportional to $1/\Gamma_t$ as the leading term in the denominator of eq. (9) for the free quark Green function). This divergent term is of the same nature as the divergence in the P wave amplitude discussed in Section 3.2. An accurate calculation of this term can be done only within the relativistic approximation. In contrast to the P wave production this term is parametrically suppressed above the threshold in comparison to the nonrelativistic continuum contribution at least by the factor $\sqrt{\Gamma_t/m_t}$ at $E \sim 0$ and can be safely omitted. However, it becomes important below the resonance region when the nonrelativistic contribution becomes small. Moreover, the denominator in the right hand side of eq. (9) decreases rapidly below the ground state pole. Therefore a small uncertainty in the numerator would lead to a large uncertainty in the function $\Phi(k)$ and a reliable estimate of its numerical value is not possible in this region within the nonrelativistic approximation. Strictly speaking the accurate determination of the function Φ below the ground state pole requires the calculation of the relativistic $O(\Gamma_t)$ contribution to the S wave cross section (the denominator of eq. (9)) which is not usually considered since it does not lead to the divergence in the nonrelativistic expression.

4 Discussion.

The results of the numerical analysis for the physical observables based on the obtained analytical expressions are plotted in Figs. 1-4.

The constant \tilde{c}_2^{++} appearing in the hard coefficient $C^{++}(\alpha_s)$ in the $O(\alpha_s^2)$ order remains unknown. The calculation of this parameter is necessary for the formal completion of the NNLO analysis. To find its numerical value one has to compute the $O(\alpha_s^2)$ perturbative QCD correction to the $\gamma\gamma$ cross section near the threshold in the formal limit $\alpha_s \ll \beta \ll 1$ and compare it with $O(\alpha_s^2)$ term in eq. (20). In the case of e^+e^- annihilation, however, the analogous contribution parameterized by \tilde{c}_2^v is relatively small (about 10% of the total NNLO correction) and the correction to the physical observables in NNLO is saturated with the soft part of the total contribution determined by the corrections to the parameters of the nonrelativistic Green function. Thus one can reasonably hope that the similar situation can also take place for $\gamma\gamma$ collisions. However the importance of this parameter for physical observables is not crucial, it affects only the overall normalization of the cross sections. For example, it does not shift the position of the resonance which is an important characteristic of the production and does not enter the ratio $R^{++}(E)/R^{++}(0)$. For the numerical analysis of the cross section R^γ we set $\tilde{c}_2^{++} = 0$.

In our approach we deal with the soft corrections by summing them into the energy denominators of the discrete part of the Green function. In other words we treat the soft corrections as effective corrections to the parameters of the Green function written in a fixed functional form. The same approach has been advocated in refs. [22, 27, 29, 30, 56] where all the corrections to the Green function have been found (numerically or analytically) in the form (24). In ref. [26], however, a part of the NNLO corrections has not been resummed to the energy denominators of the discrete part of the Green function. On the other hand, in refs. [27, 29, 30, 56] the Schrödinger equation (1) has been solved numerically, *i.e.* the NLO and NNLO correction to the Coulomb Hamiltonian have been taken into account effectively

in all orders of the nonrelativistic series (13) for the Green function while we work strictly in NNLO. Our formulae reproduce the numerical result for R^v of the most recent numerical analysis [29, 30, 56] with 1% – 3% accuracy that can be assigned to the contribution of the higher iterations of the NLO and NNLO corrections to the potential in eq. (13) beyond NNLO.

For the total cross sections which are dominated by S wave contribution we find the typical size of the NNLO corrections to be of the order of 20% in the overall normalization of the cross sections and $\sim 40\%$ in the resonance energies expressed in terms of the top quark pole mass, *i.e.* of the order of the NLO ones (see Fig. 1). Though the inclusion of the NLO corrections leads to a considerable stabilization of the theoretical results for the cross sections against changing the normalization point, the NNLO corrections do not lead to better stability as compared to NLO. In the overall normalization of the cross sections the NLO and NNLO corrections cancel each other to a large extent while the NLO and NNLO corrections to the resonance energies are of the same sign and shift the resonance farther from the threshold. They also make the peak more distinguishable which is the main difference between the leading Coulomb and NNLO approximations.

The leading order approximation for R^e and R^γ cross sections are the same up to the normalization factor $2q_t^2$. Up to the overall factor the difference between the cross sections is determined by NNLO QCD and relativistic corrections (see Fig. 2). Above the threshold this difference is determined by the difference between B^{++} and B^v coefficients and between P wave contributions to eqs. (2, 3) *i.e.* by the pure relativistic corrections. Below the threshold in the resonance region this difference is determined also by A^i coefficients and is quite sensitive to the value of α_s .

Though using an infrared safe mass parameter instead of the pole mass improves the convergence of the series for the resonance energies it does not affect the huge NNLO corrections to the cross sections normalization. Moreover, it is not clear if there exist physically

motivated mass and strong coupling parameters providing fast uniform convergence of the perturbative expansion for the cross sections in the threshold region. The absence of such a parameterization would mean the unavoidable significance of the high orders terms of the threshold expansion. Some high order effects have been already considered in the literature. The leading logarithmic corrections related to the renormalization group evolution of the hard coefficient C^v have been computed [22]. The corresponding corrections to the R^v cross section are $\pm 5\%$. In ref. [29] the running of the strong coupling constant has been taken into account by introducing the energy dependent soft normalization point of α_s entering the Coulomb potential in the numerical solution of the Schrödinger equation. The resummation of the renormalization group logarithms has an essential (up to 10%) effect in the resonance region and reduces the normalization scale dependence of the result. Furthermore, the effect of retardation which introduces a new type of contributions absent in NLO and NNLO has been analyzed for the low lying resonances [25]. The characteristic scale of the leading ultrasoft contribution was found to be about -5% for the square of the ground state wave function at the origin and $+100$ MeV for the ground state pole position.

The result for the axial coupling contribution to $e^+e^- \rightarrow t\bar{t}$ cross section is in a good agreement with the numerical analysis of ref. [28]. Up to the trivial normalization this contribution coincides with the cross section R^{+-} (Fig. 3). Numerically it does not exceed 2% of the total cross section and less than the uncertainty due to the normalization scale dependence.

The cross section R^{+-} and the function $\Phi(k)$ obtain no contribution from the ground state resonance and, therefore they are rather smooth because the top quark width smears the higher resonance contributions very efficiently (Figs. 3, 4). These quantities is rather insensitive to a variation of the normalization scale. A typical NLO correction to R^{+-} is about 10% while the one to $\Phi(k)$ is about 15% (the corrections to the forward-backward asymmetry and top quark polarization include also the hard normalization factors which have

not been included to $\Phi(k)$ itself and the nonfactorizable corrections discussed in Section 2.4). Our result for the function $\Phi(k)$ (Fig. 4) is in a good agreement with the results of numerical analysis [5, 6] for the energies above the ground state resonance. There is some discrepancy between the results below the resonance. However the reliable estimate of the function Φ is not possible in this region with the pure nonrelativistic treatment of the top quark width as has been explained in Section 3.3.

The final remark of this section concerns the optimal choice of the normalization and factorization scales. The hard scale appears in the hard coefficients as $\ln(m_t/\mu_h)$ *i.e.* the typical hard scale of the problem is the top quark mass. Though in a fixed order of the perturbative expansion the hard coefficients do not depend on μ_h one can put $\mu_h \sim m_t$ to minimize the potentially large logarithmic contributions of the higher order terms. In practice the NNLO results are almost independent of μ_h when $\mu_h \sim m_t$. On the other hand the requirement of convergence of the perturbative expansion around the Coulomb Green function restricts the allowed range for the choice of a soft normalization point which can be used for reliable estimates. The soft physical scale of the problem is determined by the natural infrared cutoff related to the top quark width $\sqrt{m_t\Gamma_t}$ that measures the distance to the nearest singularity in the complex energy plane and/or by the characteristic scale of the Coulomb problem λ *i.e.* $\mu_s \sim 15$ GeV. Both scales are rather close to each other for the case of top quark that makes possible a uniform description of both perturbative QCD and Coulomb resonance effects. Indeed, for $\mu_s \sim 15$ GeV the soft NLO correction, for example, to the energy level (25) reaches its minimal magnitude. However, at this scale the NNLO correction exceeds the NLO one and the series for the energy levels seems to diverge. Moreover, for such a low soft normalization point the NNLO corrections to the wave function at the origin which cannot be dumped by the quark mass redefinition become uncontrollable. This is not surprising since the normalization scale is defined in a rather artificial $\overline{\text{MS}}$ scheme that has little to do with peculiarities of $t\bar{t}$ physics and there is no

reason for a literal coincidence of μ_s parameter with any physical scale of the process. The relative weight of the NNLO correction to the Green function as well as the dependence of the cross sections on μ_s is stabilized at $\mu_s \gtrsim 40$ GeV which can be considered as an optimal choice of the soft normalization point. The price one pays for using different soft and hard normalization scales is the incomplete cancelation of the factorization scale dependence but this effect is suppressed by an additional power of α_s . Another source of the dependence on the factorization scale is the factorized form (4, 6) of the cross sections where some higher order μ_f -dependent terms are kept. The numerical analysis, however, shows that the results are rather insensitive to the factorization scale chosen in the region $\mu_f \sim m_t$.

5 Conclusion

The basic observables of the top quark pair production in e^+e^- annihilation and $\gamma\gamma$ collision have been considered in the threshold region. The threshold effects are described by three universal functions related to the S , P wave production and $S - P$ wave interference which have been computed analytically within (potential) NRQCD. An explicit analytical expression for the soft part of the NNLO corrections to the total cross section has been obtained. The $e^+e^- \rightarrow t\bar{t}$ threshold cross section has been obtained in NNLO in the closed form including the contribution due to the top quark axial coupling. The forward-backward asymmetry of the quark-antiquark pair production in e^+e^- annihilation and top quark polarization in both processes have been computed analytically up to NLO. The running of the strong coupling constant and the finite top quark width effects in the P wave production and $S - P$ wave interference have been taken into account properly within the analytical approach.

In combination, these uncorrelated observables form an efficient tool for investigating quark interactions. As independent sources they can also be used for determination of the theoretical uncertainty in the numerical values of the strong coupling constant α_s , the top

quark mass, and the top quark width extracted from the experimental data on top-antitop production.

The high order corrections turn out to be relatively large for all observables and important for the accurate description of the top quark physics near production threshold.

Acknowledgments

This work is partially supported by Volkswagen Foundation under contract No. I/73611 and Russian Fund for Basic Research under contract No. 97-02-17065. The work of A.A.Penin is supported in part by the Russian Academy of Sciences Grant No. 37. The present stay of A.A.Pivovarov in Mainz, where the paper has been completed, was made possible due to Alexander von Humboldt fellowship. We are thankful to K. Melnikov and A. Czarnecki [57] for pointing out an error in the partial wave decomposition of R^{++} in the previous version of this paper.

References

- [1] V.S.Fadin and V.A.Khoze, Pis'ma Zh.Eksp.Teor.Fiz. **46**(1987)417;
Yad.Fiz. **48**(1988)487.
- [2] V.S.Fadin and V.A.Khoze, Yad.Fiz. **93**(1991)1118;
I.I.Bigi, V.S.Fadin and V.A.Khoze, Nucl.Phys. **B377**(1992)461;
I.I.Bigi, F.Gabbiani and V.A.Khoze, Nucl.Phys. **B406**(1993)3;
J.H.Kühn, E. Mirkes and J.Steegborn, Z.Phys. **C57**(1993)615.
- [3] W.Kwong, Phys.Rev. **D43**(1991)1488;
M.J.Strassler and M.E.Peskin, Phys.Rev. **D43**(1991)1500;
M.Jezabek, J.H.Kühn and T.Teubner, Z.Phys. **C56**(1992)653;
Y.Sumino *et al.*, Phys.Rev. **D47**(1993)56.

- [4] E.Accomando *et al.*, Phys.Rep. **299**(1998)1.
- [5] H.Murayama and Y.Sumino Phys.Rev. **47**(1993)82;
- [6] R.Harlander, M.Jezabek, J.H.Kühn and T.Teubner, Phys.Lett. **B346**(1995)137.
- [7] V.S.Fadin, V.A.Khoze and M.I.Kotsky, Z.Phys **C64**(1994)45.
- [8] W.E.Caswell and G.E.Lepage, Phys.Lett. **B167**(1986)437;
G.E.Lepage *et al.*, Phys.Rev. **D46**(1992)4052;
G.T.Bodwin, E.Braaten and G.P.Lepage, Phys.Rev. **D51**(1995)1125.
- [9] A.V.Manohar, Phys.Rev. **D56**(1997)230.
- [10] M.Luke and A.V.Manohar, Phys.Rev. **D55**(1997)4129.
- [11] B.Grinstein and I.Z.Rothstein, Phys.Rev. **D57**(1998)78.
- [12] M.Luke and M.J.Savage, Phys.Rev. **D57**(1998)413.
- [13] A.Pineda and J.Soto, Nucl.Phys.Proc.Suppl. **64**(1998)428.
- [14] M. Beneke and V.A. Smirnov, Nucl.Phys. **B522**(1998)321.
- [15] P.Labelle, Phys.Rev. **D57**(1998)093013.
- [16] H.W.Griesshammer, Preprint **UW-98-22**, hep-ph/9810235.
- [17] A.H.Hoang, Phys.Rev. **D56**(1997)5851.
- [18] J.H.Kühn, A.A.Penin and A.A.Pivovarov, Nucl.Phys. **B534**(1998)356.
- [19] A.A.Penin and A.A.Pivovarov, Phys.Lett. **B435**(1998)413.
- [20] K.Melnikov and A.Yelkhovsky, Phys.Rev. **D59**(1999)114009.
- [21] A.A.Penin and A.A.Pivovarov, Nucl.Phys. **B549**(1999)217.

- [22] M.Beneke, A.Singer and V.A.Smirnov, Phys.Lett. **B454**(1999)137.
- [23] M.Beneke and A.Singer, Preprint **CERN-TH/99-163**, hep-ph/9906475.
- [24] A.H.Hoang, Preprint **CERN/TH 99-152**, hep-ph/9905550.
- [25] B.A.Kniehl and A.A.Penin, Preprint **DESY 99-099**, hep-ph/9907489.
- [26] A.H.Hoang and T.Teubner, Phys.Rev. **D58**(1998)114023.
- [27] K.Melnikov and A.Yelkhovsky, Nucl.Phys. **B528**(1998)59.
- [28] J.H.Kühn and T.Teubner, Eur.Phys.J. **C9**(1999)221.
- [29] T.Nagano, A.Ota and Y.Sumino, Phys.Rev. **D60**(1999)114014.
- [30] A.H.Hoang and T.Teubner, Phys.Rev. **D60**(1999)114027.
- [31] A.A.Penin and A.A.Pivovarov, Nucl.Phys. **B550**(1999)375.
- [32] A.Czarnecky and K.Melnikov, Phys.Rev.Lett. **80**(1998)2531.
- [33] M.Beneke, A.Singer and V.A.Smirnov, Phys.Rev.Lett. **80**(1998)2535.
- [34] A. Pineda and J. Soto, Phys.Lett. **B420**(1998)391, Phys.Rev. **D59**(1999)016005.
- [35] A. Czarnecki, K. Melnikov and A. Yelkhovsky, Phys.Rev. **A59**(1999)4316.
- [36] J.H.Kühn, “*Theory of the top quark production and decay*”, Lectures given at XXXIII SLAC Summer Institute on Particle Physics “*The Top Quark and the Electroweak Interaction*”
- [37] R.Karplus and A.Klein Phys.Rev. **87**(1952)848;
G.Källen and A.Sarby, K.Dan.Vidensk.Selsk.Mat.-Fis.Medd. **29**(1955), N17, 1;
R.Barbieri *et al.*, Phys.Lett. **B57**(1975)535.

- [38] L.J.Reinders, H.R.Rubinstein and S.Yazaki, Nucl.Phys. **B181**(1981)109;
J.Jérzak, E.Laemann and P.M.Zerwas, Phys.Rev. **D25**(1982)1218.
- [39] I.Harris and L.M.Brown, Phys.Rev. **105**(1957)1656;
R.Barbieri *et al.*, Nucl.Phys. **B154**(1979)535.
- [40] R.Barbieri *et al.*, Nucl.Phys. **B192**(1981)61;
J.H.Kühn and P.M.Zerwas, Phys.Rep. **B167**(1988)321.
- [41] A.A. Pivovarov, Phys.Rev. **D47**(1993)5183.
- [42] B.Grzadkowski *et al.* , Nucl.Phys. **B281**(1987)18;
R.J.Guth and J.H.Kühn, Nucl.Phys. **B368**(1992)38;
W.Beenakker, W.Hollik and Van der Mark, Nucl.Phys. **B365**(1991)24.
- [43] A.Denner, S.Dittmaier and M.Strobel, Phys.Rev. **D53**(1996)44.
- [44] B.M.Chibisov and M.V.Voloshin, Mod.Phys.Lett. **A13**(1998)973.
- [45] V.S.Fadin, V.A.Khoze and A.D.Martin, Phys.Rev. **D49**(1994)2247;
K.Melnikov and O.Yakovlev, Phys.Lett. **B324**(1994)217.
- [46] K. Fujii, T.Matsui and Y.Sumino, Phys.Rev. **D50**(1994)4341;
R.Harlander, M.Jezabek, J.H.Kühn and M.Peter, Z.Phys. **C73**(1997)477;
M.Peter and Y.Sumino, Phys.Rev. **D57**(1998)6912.
- [47] S.N.Gupta and S.F.Radford, Phys.Rev. **D24**(1981)2309; Phys.Rev.
D25(1982)3430 (Erratum);
S.N.Gupta, S.F.Radford and W.W.Repko, Phys.Rev. **D26**(1982)3305.
- [48] L.D.Landau and E.M.Lifshitz, Relativistic Quantum Theory, Part 1 (Pergamon, Oxford,
1974).

- [49] W.Fisher, Nucl.Phys. **B129**(1977)157;
A.Billoire, Phys.Lett. **B92**(1980)343.
- [50] M.Peter, Phys.Rev.Lett. **78**(1997)602; Nucl.Phys **B501**(1997)471;
Y.Schröder, Phys.Lett. **B447**(1999)321.
- [51] A.H.Hoang, Phys.Rev. **D56**(1997)7276.
- [52] K.A.Ispiryan *et al.*, Yad.Fiz. **11**(1970)1278.
- [53] A.Pineda and F.J.Yndurain, Phys.Rev. **D58**(1998)094022.
- [54] M.Beneke and V.M.Braun Nucl.Phys. **B426**(1994)301;
I.I.Bigi *et al.*, Phys.Rev. **D50**(1994)2234.
- [55] M.B.Voloshin, Nucl.Phys. **B154**(1979)365;
H.Leutwyler, Phys.Lett. **B98**(1981)447.
- [56] O.Yakovlev, Phys.Lett. **B457**(1999)170.
- [57] A.Czarnecki and K.Melnikov, Preprint **SLAC-PUB-8972**, hep-ph/0108233.

Appendix.

A. The correction $\Delta_2^{(2)}G$ due to the Δ_2V part of the potential has the form [18]

$$\begin{aligned}
\Delta_2^{(2)}G &= \left(\frac{\alpha_s}{4\pi}\right)^2 \frac{C_F \alpha_s m_t^2}{4\pi} \left(\sum_{m=0}^{\infty} F(m)^2 \left((m+1) \left(C_0^2 + L(k)C_1^2 + L(k)^2 C_2^2 \right) \right. \right. \\
&\quad \left. \left. + (m+1)\Psi_1(m+2) \left(C_1^2 + 2L(k)C_2^2 \right) + K(m)C_2^2 \right) \right. \\
&\quad \left. + 2 \sum_{m=1}^{\infty} \sum_{n=0}^{m-1} F(m)F(n) \left(-\frac{n+1}{m-n} \left(C_1^2 + 2L(k)C_2^2 \right) + K(m,n)C_2^2 \right) \right. \\
&\quad \left. + 2 \sum_{m=0}^{\infty} F(m) \left(C_0^2 + L(k)C_1^2 + (L(k)^2 + J(m))C_2^2 - (2\gamma_E + \Psi_1(m+1)) \left(C_1^2 + 2L(k)C_2^2 \right) \right) \right)
\end{aligned}$$

$$+L(k)C_0^2 + \left(-\gamma_E L(k) + \frac{1}{2}L(k)^2\right) C_1^2 + I(k)C_2^2$$

where

$$L(k) = \ln\left(\frac{\mu_s}{2k}\right)$$

$$K(m) = (m+1) \left(\Psi_1(m+2)^2 - \Psi_2(m+2) + \frac{\pi^2}{3} - \frac{2}{(m+1)^2} \right) - 2(\Psi_1(m+1) + \gamma_E),$$

$$K(m, n) = 2\frac{n+1}{m-n} \left(\Psi_1(m-n) - \frac{1}{n+1} + 2\gamma_E \right) + 2\frac{m+1}{m-n} (\Psi_1(m-n+1) - \Psi_1(m+1)),$$

$$J(m) = 2(\Psi_1(m+1) + \gamma_E)^2 + \Psi_2(m+1) - \Psi_1(m+1)^2 + 2\gamma_E^2,$$

$$I(k) = \left(\gamma_E + \frac{\pi^2}{6} \right) L(k) - \gamma_E L(k)^2 + \frac{1}{3}L(k)^3.$$

The correction $\Delta_2^{(1)}G$ due to the second iteration of $\Delta_1 V$ term [19]

$$\begin{aligned} \Delta_2^{(1)}G &= \left(\frac{\alpha_s}{4\pi}\right)^2 \frac{(C_F \alpha_s)^2 m_t^3}{4\pi} \frac{m_t^3}{2k} \left(\sum_{m=0}^{\infty} H(m)^3 (m+1) \right. \\ &\quad \left. (C_0^1 + (\Psi(m+2) + L(k)) C_1^1)^2 \right. \\ &\quad - 2 \sum_{m=1}^{\infty} \sum_{n=0}^{m-1} \frac{n+1}{m-n} C_1^1 \left(H(m)^2 H(n) \left(C_0^1 + \left(\Psi(m+2) + L(k) - \frac{1}{2} \frac{1}{m-n} \right) C_1^1 \right) \right. \\ &\quad \left. \left. + H(m) H(n)^2 \left(C_0^1 + \left(\Psi(n+2) + L(k) - \frac{1}{2} \frac{n+1}{(m-n)(m+1)} \right) C_1^1 \right) \right) \right. \\ &\quad \left. + 2(C_1^1)^2 \left(\sum_{m=2}^{\infty} \sum_{l=1}^{m-1} \sum_{n=0}^{l-1} H(m) H(n) H(l) \frac{n+1}{(l-n)(m-n)} \right. \right. \\ &\quad \left. \left. + \sum_{m=2}^{\infty} \sum_{n=1}^{m-1} \sum_{l=0}^{n-1} H(m) H(n) H(l) \frac{l+1}{(n-l)(m-n)} \right. \right. \\ &\quad \left. \left. + \sum_{n=2}^{\infty} \sum_{m=1}^{n-1} \sum_{l=0}^{m-1} H(m) H(n) H(l) \frac{(l+1)(m+1)}{(n+1)(n-l)(n-m)} \right) \right) \end{aligned}$$

where

$$H(m) = \frac{1}{m+1-\nu}$$

B. We define dimensionally regularized value of the Coulomb Green function at the origin directly through the relation

$$G_C^{d.r.}(0, 0, k) = \int d^d p \tilde{G}(p, k)$$

with $d = 3 - 2\varepsilon$. Using the following representation of the momentum space Green function

$$\tilde{G}(p, k) = \frac{m_t}{8\pi^3} \int_0^\infty \left(\frac{1+t}{t}\right)^\nu dt \frac{4k^2(1+2t)}{(p^2 + k^2(1+2t))^2}$$

one obtains

$$G_C^{d.r.}(0, 0, k) = \frac{m_t k}{2\pi} \left(\frac{\mu_f}{k}\right)^{2\varepsilon} \int_0^\infty \left(\frac{1+t}{t}\right)^\nu \frac{dt}{(1+2t)^{2\varepsilon}}$$

where we omit inessential factors related to the precise definition of integration measure in d dimensions. These factors lead to the multiplication of the Green function with an additional quantity $1 + O(\varepsilon)$ and can be taken into account by the redefinition of μ_f scale. The integral in the right hand side of this equation is

$$\int_0^\infty \left(\frac{1+t}{t}\right)^\nu \frac{dt}{(1+2t)^{2\varepsilon}} = 2^{-2\varepsilon} B(-1 + 2\varepsilon, 1 - \nu) {}_2F_1(2\varepsilon, -1 + 2\varepsilon; 2\varepsilon - \nu; \frac{1}{2})$$

where $B(z, w)$ is the Euler B -function and ${}_2F_1(a, b; c; z)$ is the hypergeometric function. Upon expanding the above expression in ε around $\varepsilon = 0$ one arrives at the final result for the dimensionally regularized Coulomb Green function. The factorization scale μ_f in eq. (17) is chosen in such a way that it is true as written. Note that the Green function regularized in this way does not automatically match the hard coefficient computed in $\overline{\text{MS}}$ scheme of the orthodox dimensional regularization [32, 33].

C. The NNLO corrections to the square of the Coulomb 3S_1 and 1S_0 heavy quark bound state wave function at the origin have the form [21]

$$\Delta_{k^2} \psi_{0m}^2 = B^i \frac{C_F^2 \alpha_s^2}{4(m+1)^2},$$

$$\Delta_{\Delta^2, NA, BF} \psi_{0m}^2 = -C_F^2 \alpha_s^2 \left(\frac{15}{8} \frac{1}{(m+1)^2} + \left(\frac{5 - A^i}{2} + \frac{C_A}{C_F} \right) \left(-\ln \left(\frac{\mu_f(m+1)}{\lambda} \right) \right) \right)$$

$$\begin{aligned}
& +\gamma_E + \Psi_1(m+1) - \frac{1}{(m+1)} \Big) \Big), \\
\Delta_2^{(2)} \psi_{0m}^2 &= \left(\frac{\alpha_s}{4\pi} \right)^2 \left(3(C_0^2 + \bar{L}(m)C_1^2 + \bar{L}(m)^2 C_2^2) + (-1 - 2\gamma_E + \frac{2}{m+1} + \Psi_1(m+2)) \right. \\
& - 2(m+1)\Psi_2(m+1))(C_1^2 + 2\bar{L}(m)C_2^2) + \left(\frac{K(m)}{m+1} + 2K(m) - 2\Psi_1(m+2) \right. \\
& \left. \left. + 2 \sum_{n=0}^{m-1} \frac{m+1}{(n-m)(n+1)} K(m,n) + 2 \sum_{n=m+1}^{\infty} \frac{m+1}{(n-m)(n+1)} K(n,m) \right) C_2^2 \right), \\
\Delta_2^{(1)} \psi_{0m}^2 &= \left(\frac{\alpha_s}{4\pi} \right)^2 \left(3(C_0^1 + (\bar{L}(m) + \Psi_1(m+2))C_1^1)^2 \right. \\
& + 2C_1^1 \left(\sum_{n=0}^{m-1} \frac{(n+1)(m+1)}{(n-m)^3} \left(C_0^1 + \left((\bar{L}(m) + \Psi_1(n+2)) + \frac{1}{2} \frac{n+1}{(n-m)(m+1)} \right) C_1^1 \right) \right. \\
& \left. \left. - \sum_{n=m+1}^{\infty} \frac{(m+1)^2}{(n-m)^3} \left(C_0^1 + \left((\bar{L}(m) + \Psi_1(n+2)) - \frac{1}{2} \frac{1}{n-m} \right) C_1^1 \right) \right) \right) \\
& + 2C_1^1 \left(C_0^1 + (\bar{L}(m) + \Psi_1(m+2)) C_1^1 \right) \left(-\frac{5}{2} + \sum_{n=0}^{m-1} \frac{n+1}{(n-m)^2} U(m,n) \right. \\
& \left. - \sum_{n=m+1}^{\infty} \frac{m+1}{(n-m)^2} U(m,n) \right) + 2(C_1^1)^2 \left(\frac{1}{2} - \sum_{n=0}^{m-1} \frac{n+1}{(n-m)^2} + \sum_{n=m+1}^{\infty} \frac{m+1}{(n-m)^2} \right. \\
& \left. + \frac{1}{2} \sum_{n=0}^{m-1} \frac{n+1}{(n-m)^3} U(m,n) + \frac{1}{2} \sum_{n=m+1}^{\infty} \frac{(m+1)^2}{(n-m)^3(n+1)} U(m,n) \right) \\
& + \sum_{n=1}^{m-1} \sum_{l=0}^{n-1} \left(\frac{(l+1)(n+1)}{(n-m)^2(l-m)^2} - \frac{(l+1)(m+1)}{(n-m)^2(l-m)(n-l)} - \frac{(l+1)(m+1)}{(l-m)^2(n-m)(n-l)} \right) \\
& + \sum_{n=m+1}^{\infty} \sum_{l=0}^{m-1} \left(-\frac{(l+1)(m+1)}{(n-m)^2(l-m)^2} + \frac{(l+1)(m+1)^2}{(n-m)^2(l-m)(n-l)(n+1)} \right. \\
& \left. - \frac{(l+1)(m+1)}{(l-m)^2(n-m)(n-l)} \right) + \sum_{n=2}^{\infty} \sum_{l=m+1}^{n-1} \left(\frac{(m+1)^2}{(n-m)^2(l-m)^2} \right. \\
& \left. \left. + \frac{(l+1)(m+1)^2}{(n-m)^2(l-m)(n-l)(n+1)} + \frac{(m+1)^2}{(l-m)^2(n-m)(n-l)} \right) \right) \Big)
\end{aligned}$$

where $\bar{L}(m) = L(\lambda/(m+1))$ and

$$U(m,n) = 3 + \frac{n+1}{m+n+2} - 2 \frac{(n+1)^2}{(n-m)(n+m+2)}$$

D. The NNLO corrections to the Coulomb 3S_1 and 1S_0 heavy quark bound state energy levels [20, 21, 53]

$$\begin{aligned}\Delta_{\Delta^2, NA, BF} E_{0m} &= \frac{C_F^2 \alpha_s^2}{(m+1)} \left(\frac{C_A}{C_F} + \frac{5-A^i}{2} - \frac{11}{16} \frac{1}{(m+1)} \right), \\ \Delta_2^{(2)} E_{0m} &= 2 \left(\frac{\alpha_s}{4\pi} \right)^2 \left(C_0^2 + \bar{L}(m) C_1^2 + \bar{L}(m)^2 C_2^2 + \Psi_1(m+2)(C_1^2 + 2\bar{L}(m)C_2^2) \right. \\ &\quad \left. + \frac{K(m)}{(m+1)} C_2^2 \right), \\ \Delta_2^{(1)} E_{0m} &= \left(\frac{\alpha_s}{4\pi} \right)^2 \left((C_0^1 + (\bar{L}(m) - 2 + \Psi_1(m+2))C_1^1) (C_0^1 + (\bar{L}(m) + \Psi_1(m+2))C_1^1) \right. \\ &\quad \left. + \left(\frac{2}{(m+1)} (\gamma_E + \Psi_1(m+2)) - 2\Psi_2(m+1) - (m+1)\Psi_3(m+1) \right) (C_1^1)^2 \right),\end{aligned}$$

Figure captions

Fig. 1. The normalized cross section $R^v(E)$ in the leading order (solid lines), NLO (bold dotted lines) and NNLO (bold solid lines) for $m_t = 175$ GeV, $\Gamma_t = 1.43$ GeV, $\alpha_s(M_Z) = 0.118$ and $\mu_s = 50$ GeV, 75 GeV and 100 GeV. The dotted line corresponds to the result in Born approximation.

Fig. 2. The normalized cross sections $R^e(E)$ (dotted lines) and $R^\gamma(E)$ (solid lines) in NNLO for $\tilde{c}_2^{++} = 0$, $m_t = 175$ GeV, $\Gamma_t = 1.43$ GeV, $\alpha_s(M_Z) = 0.118$, $\sin^2 \theta_W = 0.232$, $M_Z = 91.2$ GeV and $\mu_s = 50$ GeV, 75 GeV and 100 GeV.

Fig. 3. The normalized cross section $R^{+-}(E)$ in the leading order (dotted lines) and NLO (bold solid lines) for $m_t = 175$ GeV, $\Gamma_t = 1.43$ GeV, $\alpha_s(M_Z) = 0.118$ and $\mu_s = 50$ GeV, 75 GeV and 100 GeV. The solid line corresponds to the result in Born approximation.

Fig. 4. The function $\Phi(E)$ in the leading order (dotted lines) and NLO (bold solid lines) for $m_t = 175$ GeV, $\Gamma_t = 1.43$ GeV, $\alpha_s(M_Z) = 0.118$ and $\mu_s = 50$ GeV, 75 GeV and 100 GeV. The solid line corresponds to the result in Born approximation.

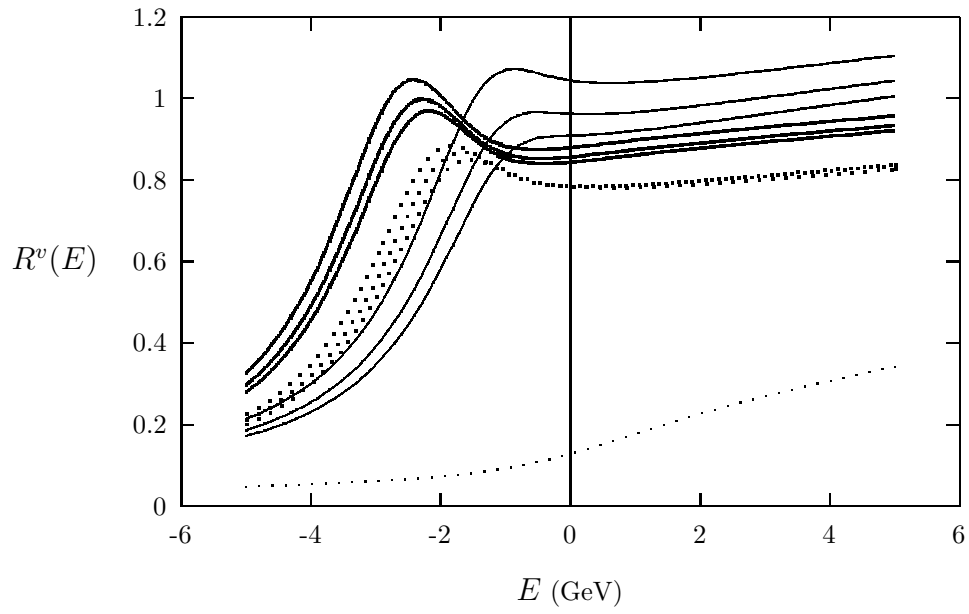


Fig. 1.

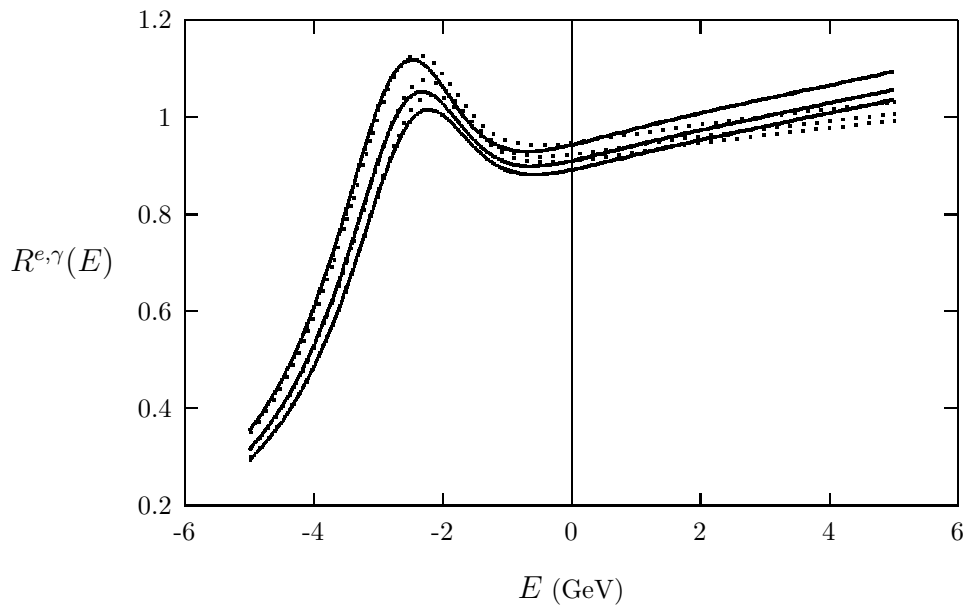


Fig. 2.

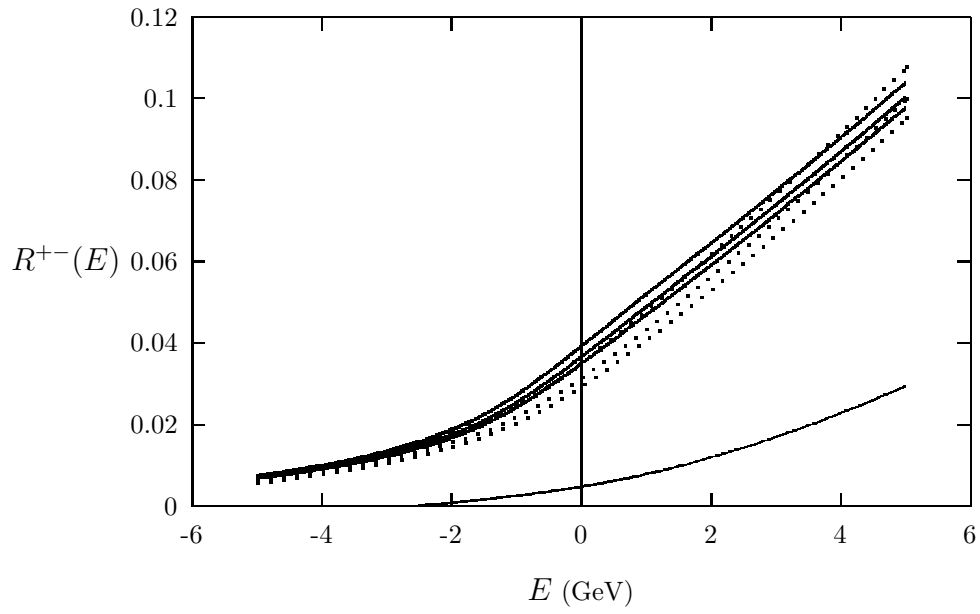


Fig. 3.

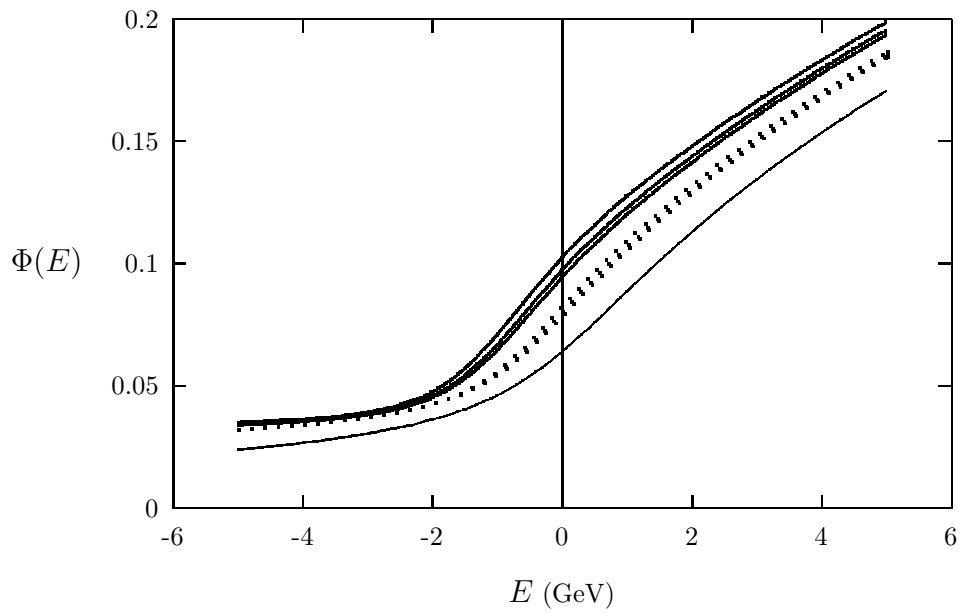


Fig. 4.